Laboratory Experiments and Modeling for Interpreting Field Studies of Secondary Organic Aerosol Formation Using an Oxidation Flow Reactor.

Initial Proposal/Grant Title: *"COLLABORATIVE RESEARCH: Study of Aerosol Sources and Processing at the GVAX Pantnagar Supersite"*

Final Technical Report

Period Covered: 15-April-2011 – 15-April-2015

February 2016

Prof. Jose-Luis Jimenez
University of Colorado
Boulder, Colorado

PREPARED FOR:
THE U.S. DEPARTMENT OF ENERGY
OFFICE OF SCIENCE
OFFICE OF BIOLOGICAL AND ENVIRONMENTAL RESEARCH
ATMOSPHERIC SYSTEMS RESEARCH PROGRAM
UNDER CONTRACT NO. DE-SC0006035

Table of Contents

List of Figures and Tables

multiple field locations.

Figure 25. Ratio of OA to excess CO vs. total photochemical age for ambient and OFR data during CalNex-LA and other campaigns for reference.

Figure 26. Comparison of OFR data with model results for evolution of OA/ΔCO vs. total photochemical age with different models for CalNex-LA.

Figure 27. Mass fraction remaining of IEPOX-SOA as a function of OH_{exp} in the OFR during the SOAS and GoAmazon2014/15 (dry season) campaigns.

Figure 28. OA enhancement vs. age for OH, O_3, and NO_3 oxidation, separated into daytime and nighttime data for the BEACHON-RoMBAS campaign.

Figure 29. Modeled fractional fates of loss of low-volatility organic compounds (LVOCs) to OFR walls, condensation to aerosols, reaction with OH to produce volatile products, or exiting the OFR to be lost on sampling line walls as a function of photochemical age (BEACHON-RoMBAS campaign).

Figure 30. Comparison of OA enhancement from OH oxidation using the OFR185 and OFR254 methods (BEACHON-RoMBAS campaign) vs photochemical age (day/night).

Figure 31. (left panel) Measured vs. predicted SOA formation from OH oxidation of ambient air in an OFR using the OFR185 method (BEACHON-RoMBAS campaign). VOCs only used for SOA prediction (right panel) Same data as shown in left panel except only including data when there was temporal overlap of measurements of volatility-separated semi/intermediate VOCs (S/IVOCS) using a novel TD-EIMS method (BEACHON-RoMBAS campaign). VOCs + S/IVOCs used for SOA prediction.

Figure 32. Gas/particle partitioning as a function of carbon number for measured (MOVI-HRToF-CIMS) and modeled alkanoic acids using different published $P°_{L,i}$ and ΔH_{vap} values (BEACHON-RoMBAS campaign).

Figure 33. Partitioning for bulk averaged acids binned into carbon number bins (MOVI-HRToF-CIMS) and modeled partitioning calculated using excess oxygen as different organic functional groups (BEACHON-RoMBAS campaign).

Figure 34. Measured and modeled partitioning of pinic acid determined with the MOVI-HRToF-CIMS during the BEACHON-RoMBAS field study.

Summary

This grant was originally funded for deployment of a suite of aerosol instrumentation by our group in collaboration with other research groups and DOE/ARM to the Ganges Valley in India (GVAX) to study aerosols sources and processing. Much of the first year of this grant was focused on preparations for GVAX. That campaign was cancelled due to political reasons and with the consultation with our program manager, the research of this grant was refocused to study the applications of oxidation flow reactors (OFRs) for investigating secondary organic aerosol (SOA) formation and organic aerosol (OA) processing in the field and laboratory through a series of laboratory and modeling studies. We developed a gas-phase photochemical model of an OFR which was used to 1) explore the sensitivities of key output variables (e.g., OH exposure, O_3, HO_2/OH) to controlling factors (e.g., water vapor, external reactivity, UV irradiation), 2) develop simplified OH exposure estimation equations, 3) investigate under what conditions non-OH chemistry may be important, and 4) help guide design of future experiments to avoid conditions with undesired chemistry for a wide range of conditions applicable to the ambient, laboratory, and source studies. Uncertainties in the model were quantified and modeled OH exposure was compared to tracer decay measurements of OH exposure in the lab and field. Laboratory studies using OFRs were conducted to explore aerosol yields and composition from anthropogenic and biogenic VOC as well as crude oil evaporates. Various aspects of the modeling and laboratory results and tools were applied to interpretation of ambient and source measurements using OFR. Additionally, novel measurement methods were used to study gas/particle partitioning. The research conducted was highly successful and details of the key results are summarized in this report through narrative text, figures, and a complete list of publications acknowledging this grant.

Introduction

Aerosols play a critical but poorly understood role in the Earth's climate forcing (Myhre et al., 2013), since they can affect cloud brightness, lifetime, and precipitation ("indirect effects") and they can scatter or absorb incoming solar radiation ("direct effect") (Charlson et al., 1992; Hansen et al., 1997). Both climate effects depend strongly on the aerosol concentration, size and chemical composition. Compared to the other components of the total radiative budget such as CO_2, the uncertainties associated with the effects of aerosols are very large, and account for most of the uncertainty in the latest IPCC estimates (Myhre et al., 2013) of net anthropogenic radiative forcing. In large part this uncertainty is due to the fact that aerosols, unlike well-mixed greenhouse gases, vary strongly in space and time in concentration, size, and composition. Submicron aerosols are the most active climatically, and organic aerosols (OA) represent a major fraction of their mass, with the balance composed of inorganic species, chiefly sulfate, nitrate, and ammonium, as well as black carbon (Jimenez et al., 2009). Sulfate sources and chemistry are better understood, but OA sources remain poorly characterized (Kanakidou et al., 2005; Hallquist et al., 2009; Spracklen et al., 2011; Tsigaridis et al., 2014). It has become clear in recent years that secondary organic aerosols (SOA), which are formed in the atmosphere from condensation of lower volatility oxidation products of volatile organic compounds (VOCs), dominate OA worldwide (de Gouw, 2005; Zhang et al., 2007; Jimenez et al., 2009).

Despite the importance of SOA for urban, regional and global submicron aerosols and thus human health effects and climate forcing, its sources, sinks, and rates of formation in the atmosphere are poorly understood (e.g., de Gouw and Jimenez, 2009; Hallquist et al., 2009; Tsigaridis et al., 2014). Therefore, it is not surprising that there are often major discrepancies between modeled and observed SOA concentrations in the atmosphere. For example, measured SOA loadings have been shown to be an order-of-magnitude larger than traditional models in a variety of polluted environments, such as off the coast of New England (de Gouw, 2005), Mexico City (Volkamer et al., 2006; Dzepina et al., 2009), and off the coast of East Asia (Heald et al., 2005). Many possible explanations for these large discrepancies have been put forward that involve previously unrecognized sources or mechanisms of formation (Ziemann, 2002; Kalberer et al., 2004; Kroll et al., 2005). However, when these sources are combined, models can produce excessive amounts of SOA, and our current ability to distinguish between SOA formed from different sources and remains insufficient (Lane et al., 2008; Lim et al., 2010; Ervens et al., 2011). SOA sinks are also likely underestimated (Hodzic et al., 2014; Knote et al., 2015). The inability of models to predict both SOA concentrations and degree of oxidation highlights a critical need for innovative observational approaches to constrain the processes controlling this important atmospheric component and climate forcing agent. Improving the ability of models to (a) characterize radiative forcing due to OA since preindustrial times and (b) predict the evolution of that forcing over the coming decades to centuries under a changing climate and

emissions will require a much better understanding of SOA sources and sinks, gas/particle partitioning, and atmospheric aging.

For these reasons, in order to help elucidate the factors that control SOA formation and OA processing in the atmosphere, our group has invested considerable effort in development of a field-deployable Oxidation Flow Reactor (OFR). An OFR, commonly referred to as "PAM" (Potential Aerosol Mass) flow reactor, was recently developed for rapid quantification and characterization of secondary aerosol production (Kang et al., 2007, 2011). It is designed for fast response time and to minimize wall interactions characteristic of large chambers. It employs 1-4 orders of magnitude higher OH (or O_3 or NO_3) concentrations than ambient levels for exposure times of ~5 minutes, resulting in integrated oxidant exposures equivalent of a few hours to several weeks of atmospheric oxidation. Despite the intense oxidative conditions in the OFR, SOA yields for various biogenic and anthropogenic precursor gases were shown to be similar to those of batch reactions in large environmental chambers for similar degrees of oxidation, with variations and differences mostly within the range of those observed for chamber results from different groups (Kang et al., 2007, 2011; Lambe et al., 2015). Also, the degree of oxidation of the OA produced has been shown to span values between fresh and very aged ambient OOA observations, compared to lower values commonly observed in chamber studies (Kang et al., 2007, 2011; Aiken et al., 2008; Lambe et al., 2011a). Hygroscopicity and CCN activity of SOA produced in the OFR is similar to ambient SOA and depends on the oxygen-to-carbon ratio (O:C) in the same way as atmospheric OA (Massoli et al., 2010), providing further evidence that the OFR generates SOA similar to that in the atmosphere.

Due to the short timescale and portability of this OFR, our group has pioneered its use as a field-deployable tool for studying SOA in the ambient atmosphere including development of an automated system that steps through variable degrees of oxidant exposure, records O_3, RH, and irradiation used to continuously monitor oxidant exposure, and control valves that allow for alternately sampling outflows of multiple OFRs and unperturbed ambient sampling with an AMS, SMPS, PTRMS and other instruments for gas and aerosol analysis.

We have deployed the OFR-AMS-SMPS system during multiple field and lab campaigns using OH, O_3, and NO_3 as oxidants (Li et al., 2013; Ortega et al., 2013, 2015; Palm et al., 2015, 2016a, 2016b). Results from those experiments have shown that OH-initiated oxidation of ambient air shows trends in elemental ratios similar to the atmosphere, and to ambient SOA at multiple locations, consistent with functionalization by a combination of carboxylic acid and hydroxyl addition (however favoring acid) or carboxylic acid addition with carbon-carbon fragmentation (Ng et al., 2011). Importantly, high degrees of oxidation (comparable to atmospheric observations) is achievable at the highest OH, demonstrating the ability of the OFR to generate highly aged SOA. Also, we have generally observed that with increasing OH exposure SOA enhancement increases and with increasing exposure the enhancement decreases, with net loss of OA observed at the highest exposures, due to a changing balance of

functionalization/condensation and fragmentation/evaporation.

Despite the increasing use of OFRs by our group and others in the field and laboratory, systematic characterization of the radical chemistry in OFRs had not been conducted. Thus, quantifying the degree (and type) of oxidant exposure as well as ability to assess the representativeness of the OFR chemistry to atmospheric processes had been highly uncertain or not possible until recently (work supported by this grant), potentially leading to ambiguous or inaccurate representations of OFR measurements. The work funded by this grant and described herein has consisted of a systematic approach using modeling and laboratory studies of OFRs and provided major advances in the quantification and understanding of the application of OFRs for the investigation and SOA formation and OA processing. It has helped to demonstrate the utility of using OFRs, identify potential limitations, and provide recommendations for experimental design and interpretation. Results stemming from the improved implementation and interpretation of OFR measurements will help improve our understanding of aerosol life cycle and has the potential to be applied to regional and global modeling and help reduce the uncertainties in climate forcing by aerosols and on air quality prediction – in line with the goals of the ASR program.

1. GVAX Campaign Preparations

In this section we summarize the preparations for the GVAX field campaign. Following the cancelation of the campaign, our project focus changed to laboratory experiments to aid in the interpretation of the application of the OFR SOA formation chamber to field studies, which is described next.

Figure 1. *Visit to Nainital site June 2011 where ARIES/ARM-1 annual-cycle of aerosol, gas, radiation, and meteorological measurements were underway.*

1.1 Site Visit to India (June 2011)

During June, 2011, Staff Scientist in our group, Doug Day, travelled to India for planning purposes. He traveled with Leah Williams (Aerodyne Research, Inc.), Rao Kotamarthi (Argonne Nat. Lab), Peter Daum (Brookhaven Nat. Lab), and Tim Martin (Argonne Nat. Lab). The trip included: 1) meetings at the Indian Institute of Science (IISc) in Bangalore with our contacts from the IISc (Dr. S.K. Satheesh) and Indian Space Research Organization (Drs. K. Krishnamoorthy and S. Suresh Babu), 2) visit to the ARIES/ARM-1 site in Nainital (*Fig. 1*) where an annual cycle of aerosol and radiation measurements had already begun and met contacts: Prof. Ram Sagar (ARIES), Manish Naja (ARIES), Carlos Sousa (ARM), and 3) two visits to Pantnagar University, the planned location of the winter 2012 ground supersite, to meet local contacts, survey the proposed measurement site, start identifying housing options, and identify other logistical issues (*Figs. 2-4*). Additionally, Doug took many photographs at the Nainital and Pantnagar sites to aid logistical planning. Please find pictures from the recon trip at http://tinyurl.com/reconGVAX: Pantnagar University and supersite location (88-182, 309-635); Nainital ARIES/ARM-1 (183-307). A report was prepared detailing the various aspects of the Pantnagar proposed site location including: power voltage and frequency monitoring, temperatures at difference building locations, site

Figure 2. *Doug Day (CU) and Williams (ARI) survey proposed Pantnagar supersite compound.*

Figure 3. *Surveying Pantnagar supersite compound (left background) from Physical Sciences building rooftop (proposed MAX-DOAS location). Prof. K. P. Singh (Pant. Univ), Leah Williams (ARI), and Peter Daum (Brookhaven N.L.) in forground; DOE "Cool Roof" test location in right background.*

Figure 4. *Surveying Pantnagar University library: tallest structure at University; potential location of MAX-DOAS and meteorological instrumentation.*

dimensions and distances, aerosol and gas inlet and filter sampler locations, and considerations for placement of the Volkamer group MAX-DOAS (with a focus on minimizing obstructions on the horizon).

1.2 Continuing Site/Campaign Planning and Preparation (July-December 2011)

Following the logistical planning trip to India, our group continued to prepare for the winter 2012 intensive campaign in Pantnagar, India. This included partipating in monthly, then weekly phone conferences, packing all equipment to send to Aerodyne Research, Inc (ARI; Billerica, MA) for upload into DOE-funded seatainers, coordinating shared tools/equipment, documenting all equipment and supplies and values for upload at ARI (September 2011). Doug Day and CU graduate student Brett Palm spent over a week at ARI, integrating our equipment into the instrument and supplies and storage seatainers (HR-ToF-AMS, OFR light controls and chamber, DustTrak, OPC, SMPS, thermal denuder, SO_2 monitor, O_3 monitor). See *Fig. 5* - additional pictures of the integration can be found at http://tinyurl.com/reconGVAX (745-825). Additionally in September, 2011 Doug Day participated in the ASR Fall Working Group meeting http://asr.science.energy.gov/meetings/fall-working-groups/, presented an update on the Pantnagar supersite planning on behalf of our group at the University of Colorado, and groups at ARI, University of Washington, Los Alamos Nat. Laboratory, Argonne Nat. Laboratory, and NOAA and participated in discussions about general GVAX campaign planning. The GVAX winter intensive campaign was cancelled by DOE on November 23, 2012. Following that cancellation, Doug Day and Brett Palm travelled to ARI to unintegrate our equipment and supplies from the ARI seatainers and ship them back to our laboratory.

Figure 5. *Instrument installation and packing at Aerodyne in preparation for seatainer shipment to India. Clockwise from upper left: i) installation of HR-ToF-MS in instrument seatainer, ii) Brett Palm - finished with all instrument installation, iii) all non-mounted instrumentation and supplies packed and catalogued for shipping/customs in non-instrument seatainer, and iv) Doug Day conducting final HR-ToF-AMS tests.*

2. Oxidation Flow Reactor (OFR) Lab Studies and Modeling

Following the cancelation of the GVAX campaign in India (planned for winter 2012), our project focus changed (after consultation with DOE Program managers) to laboratory experiments coupled with modeling to aid in the interpretation of the application of the oxidation flow reactors (OFR) to field studies aimed at understanding secondary organic aerosol (SOA) formation and processing, as well as to advanced analysis of the field data. Large gaps exist in our understanding of SOA formation and processing in the atmosphere which in situ field measurements of rapid oxidation have a strong potential to help clarify. However, characterization of the OFRs through laboratory experiments and modeling is a critical step required to improve and validate and improve this method as an effective tool for the study of atmospheric photochemical SOA-forming/aging processes.

2.1 Modeling Studies of Radical Chemistry in Oxidation Flow Reactors

Understanding the gas-phase oxidation chemistry within the OFR is critical to interpret OFR studies of VOC oxidation and/or SOA formation and aging in the laboratory or field. However, despite the increasing use of OFRs to study SOA formation and aging, very little systematic study of the oxidation chemistry of OFRs has been reported. Factors such as the amount and type of oxidant exposure, the reaction partners of RO_2 radicals (e.g., RO_2, HO_2, NO_x), or the effects of photolysis can affect the extent and type of chemistry occurring within an OFR. Understanding and quantifying these effects and what controls them allows for assessment of whether (and in which ways) the conditions are representative of atmospheric oxidation chemistry as well as the ability to design operating conditions to optimize the reactors to achieve targeted conditions. In particular, having a robust method for determining oxidant exposures is required in order to confidently assign aging/oxidant timescales to air sampled from the atmosphere, controlled biomass burning, combustion source studies, or synthetic mixtures in the laboratory. Errors in oxidant exposures will hinder accurate prediction of timescales for SOA formation, chemical transformation, and losses and will thus be propagated into any products used in regional or global modeling efforts. For ozone oxidation experiments, quantification of exposure is relatively straightforward as it only involves direct ozone measurements and knowledge of the flow residence time. Quantifying OH exposure is far more challenging since OH is a very short-lived radical and real-time OH measurements in the OFR are not practical.

Therefore, we have developed a kinetic model to study the radical chemistry and its sensitivities and uncertainties, developed OH exposure calibration equations, evaluated the model and calibration equations with laboratory and field measurements, and provide recommendations for operating oxidation flow reactors.

2.1.1 Modeling Radical Chemistry, Sensitivities, and OH Exposure in OFR185

To better understand the chemistry in the "OFR185" we developed a model to simulate the formation, recycling, and destruction of radicals and to allow the quantification of OH exposure

(OH_{exp}) in the reactor and its sensitivities (*Fig. 6*). The "OFR185" is a version of the OFR using primarily OH oxidation where the OH radicals are generated primarily by photolysis of H_2O ($H_2O+h\nu$ (185 nm)→OH+H) and photolysis of O_3 formed from O_2 photolysis:

$$O_2 \xrightarrow{h\nu(185\text{nm})} 2O(^3P) \xrightarrow{O_2} 2O_3 \xrightarrow{h\nu(254\text{nm})} 2O(^1D) \xrightarrow{H_2O} 2OH \quad (1)$$

Thus both the 185 nm and 254 nm emission lines from the low-pressure mercury lamps are used to generate OH within the reactor. This is in contrast to the OFR254, which produces OH via injection of externally-generated O_3 followed by photolysis by 254 nm UV light (second half of series in Reaction 1; no 185 nm light present). A sensitivity study was performed to characterize the dependence of the OH_{exp}, HO_2/OH ratio, and O_3 and H_2O_2 output concentrations on reactor parameters. OH_{exp} is strongly affected by the UV photon flux, absolute humidity, reactor residence time, and the OH reactivity (OHR) of the sampled air, and more weakly by pressure and temperature. OH_{exp} can be strongly suppressed by high external OH reactivity (OHR; NO_x, VOC, CO, SO_2, etc.), especially under low UV light conditions. The effects are external OHR become significant when it is becomes comparable to the internal OHR (e.g., *Fig. 7*). The OFR185 model outputs of OH exposure (OH_{exp}) were evaluated against laboratory calibration experiments by estimating OH_{exp} from trace gas removal and were shown to agree within a factor of 2 (*Fig. 8*). An OH_{exp} estimation equation as a function of easily measurable quantities was shown to reproduce model results within 10% (average absolute value of the relative errors) over the whole operating range of the reactor. OH_{exp} from the estimation equation was compared with measurements in several field campaigns and showed agreement within a factor of 3 (*Fig. 9*). The improved understanding of the OFR185 and quantification of OH_{exp} resulting from this work further establish the usefulness of such reactors for research studies, especially where quantifying the oxidation exposure is important. Further details of this work can be found in Li et al. (2015).

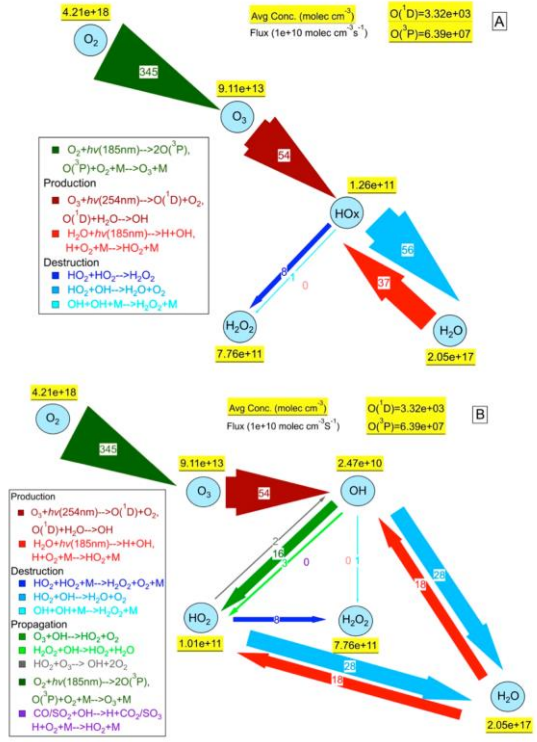

Figure 6. *Schematic of OH185 model showing reaction fluxes and concentrations of HO_x (other O_x, HO_y species) for conditions of moderate UV lamp power (40% of max) and RH (50%) at room temperature. The top scheme (A) shows HO_x as a single pool, while the bottom (B) shows OH and HO_2 separately. Fluxes are in units of 10^{10} molec cm^{-3} s^{-1}) and arrows are sized by flux (except $O_2+h\nu$ which is scaled down by x5).*

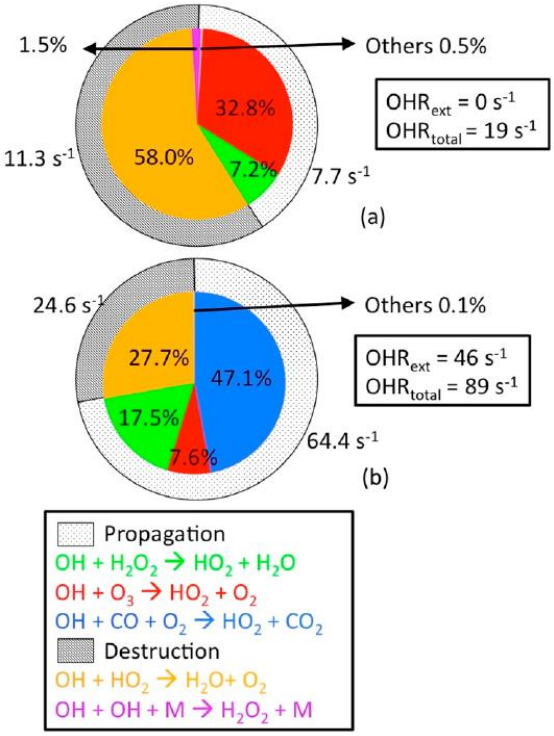

Figure 7. *Budget of OH reactivity (OHR), both "internal" and "external". (a) Fraction of total OHR for the base case (moderate conditions), without external OHR. (b) Fraction of total OHR when 46 s^{-1} of external OHR is added to the base case (via a 10 ppmv initial CO mixing ratio).*

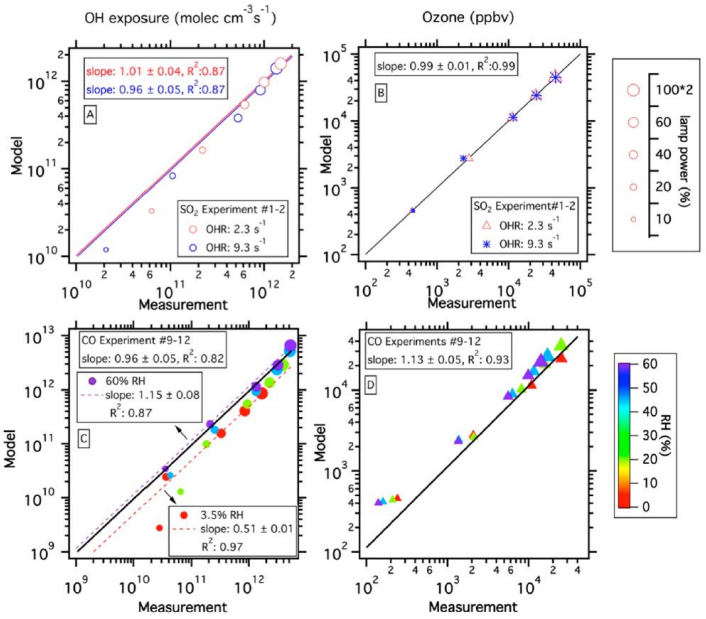

Figure 8. *Comparison between model results (y-axes) and measurements from calibration experiments (of SO_2, CO decay) for OH_{exp} (A,C) and O_3 mixing ratios (B,D) under various UV flux and humidity conditions. Panels A and B show the comparisons using SO_2 as the reactant trace gas (initial concentrations of 500 and 100 ppbv, i.e., 10 and 2 s^{-1} OHR) with different UV fluxes at 3.5% RH. Panels C and D show the comparisons using CO (initial concentration of 10 ppmv, i.e., 50 s^{-1} external OHR) at different UV fluxes and RH (color coded). Data are size-coded with lamp power settings, ranging from one lamp at 10% to two lamps at 100%. In CO experiments (C,D), the data are also color-coded with four different RH, ranging from 3.5 to 60%.*

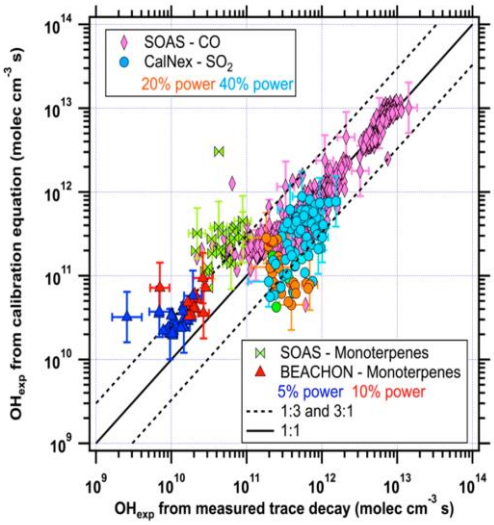

Figure 9. *OH_{exp} from the estimation equation (see text) versus OH_{exp} calculated from added/ambient tracer decay for different field studies and tracers. The uncertainty of OH_{exp} obtained from the estimation equation (vertical bars) is estimated as a factor of 2. The uncertainty of OH_{exp} calculated from tracer species decay in the field measurements (horizontal bars) was estimated for each case. On average, the uncertainties for OH_{exp} estimated from SO_2, CO, and monoterpenes are 34, 30, and 29%.*

2.1.2 Modeling HO_x Radical Chemistry, Sensitivities, Uncertainties in OFR185, OFR254

In a follow-up modeling study, we further developed the plug-flow kinetic model (described in last section) to investigate OFR properties under a very wide range of conditions applicable to both field and laboratory studies for both OFR185 and OFR254 (*Fig. 10*). This modeling shows that the radical chemistry in OFRs can be characterized as a function of UV light intensity, H_2O concentration, and total external OH reactivity (OHR_{ext}). OH exposure is decreased by added external OH reactivity (*Fig. 11*). OFR185 is especially sensitive to this effect at low UV intensity due to low primary OH production. OFR254 can be more resilient against OH suppression at high injected O_3 (e.g., 70 ppm), as a larger primary OH source from O_3, as well as enhanced recycling of HO_2 to OH, make external perturbations to the radical chemistry less significant (*Fig. 11*). However, if the external OH reactivity in OFR254 is much larger than OH reactivity from injected O_3, OH suppression can reach 2 orders of magnitude (*Fig. 14*). For a typical input of 7 ppm O_3 (OHR_{O3} = 10 s^{-1}), 10-fold OH suppression is observed at OHR_{ext} ~ 100 s^{-1} (*Fig. 11*), which is similar or lower than used in many laboratory studies (*Fig. 14*). The range of modeled OH suppression for literature experiments is consistent with the measured values except for those with isoprene. The finding on OH suppression may have important implications for the interpretation of past laboratory

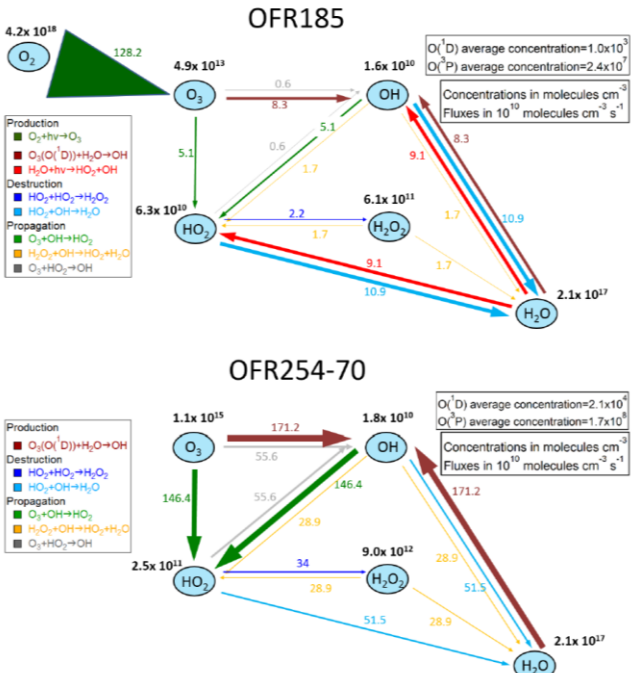

Figure 10. *Schematic of modeled chemistry for OH185 (top) and OH254 (bottom, with 70 ppb O_3 injected) showing reaction fluxes and concentrations of HO_x (other O_x, HO_y species) as in Fig. 6 and with for moderate conditions and no OHR_{ext}.*

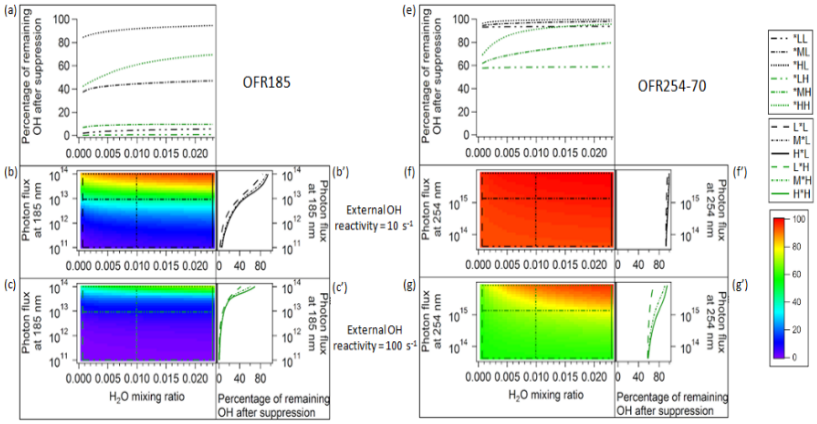

Figure 11. *Effects of external OH reactivity (OHR_{ext}) OH exposure (OH_{exp}) shown as percentage of remaining OH after suppression vs. photo flux and water vapor compared to a reference case with no OHR_{ext}. Left shows reactor using 185+254 nm UV light (OH185); Right shows reactor using 254 nm light only (OH254; 70 ppm O_3 injection). The 3-letter codes corresponds to high (H), medium (M), and low (L) water vapor, light flux, and OHR, respectively.*

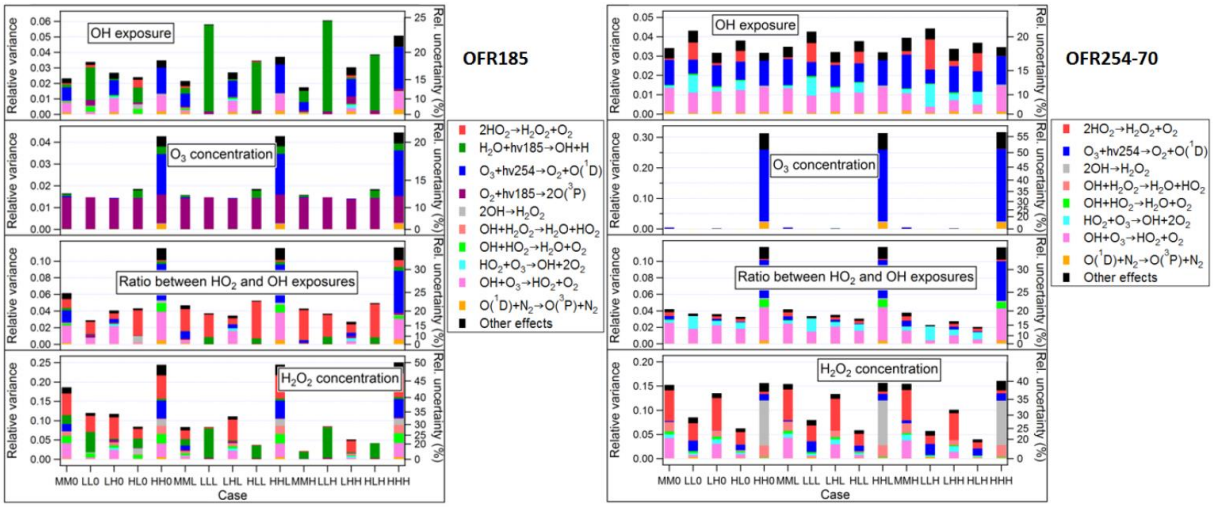

Figure 12. *Relative variances (left axes)/uncertainties (right axes) of the outputs (i.e., OH exposure, O_3 concentration, ratios between HO_2 and OH exposure, and H_2O_2 concentration) of Monte Carlo uncertainty propagation, and relative contributions of key reactions to these relative variances in typical cases in OFR185 and OFR254-70. Relative variances are shown in linear scales (left axis), while corresponding relative uncertainties, equal to relative variances' square roots, are indicated by the non-linear right axis. Only the reactions with a contribution of no less than 0.04 to at least 1 relative variance are shown.*

studies, as applying OH_{exp} measurements acquired under different conditions could lead to over a 1-order-of-magnitude error in the estimated OH_{exp} (*Fig. 14*).

As part of the modeling, the uncertainties on the model outputs due to the uncertainty in model parameters (rate constants and (partial) cross-sections) were quantified and compared to the dynamic ranges of some outputs to confirm the reliability of the results of interest (such as described above). The uncertainties of key model outputs due to uncertainty in all rate constants and absorption cross-sections in the model are within ±25% for OH_{exp} and within ±60% for other parameters (*Fig. 12*). These uncertainties are small relative to the dynamic range of outputs. Uncertainty analysis shows that most of the uncertainty is contributed by photolysis rates of O_3, O_2, and H_2O_2 and reactions of OH and HO_2 with themselves or with some abundant species, i.e., O_3 and H_2O_2.

Differences in calculated OH_{exp} due to assumptions of flow dynamics within the reactor were evaluated with the model since the base model assumes plug-flow, when in fact it has been shown to have a broader residence time distribution (Lambe et al., 2011b). OH_{exp} calculated from direct integration and estimated from SO_2 decay in the model with laminar and measured residence time distributions (RTDs) are generally within a factor of 2 from the plug-flow OH_{exp} (*Fig. 13*). However, in the models with RTDs, OH_{exp} estimated from SO_2 is systematically lower than directly integrated OH_{exp} in the case of significant SO_2 consumption (*Fig. 13*). We thus recommend using OH_{exp} estimated from the decay of the species under study when possible, to obtain the most appropriate information on photochemical aging in the OFR.

We also explored differences in the type of OHR_{ext}, i.e. the rate constant or whether an OHR compound recycled OH back to HO_2 (such as VOCs often do or CO and SO_2 always do) or permanently remove HO_x upon reaction with OH (e.g., NO_2). Using HO_x-recycling vs. destructive external OH reactivity only leads to small changes in OH_{exp} under most conditions. Changing the identity (rate constant) of external OH reactants can result in substantial changes in OH_{exp} due to different reductions in OH suppression as the reactant is consumed.

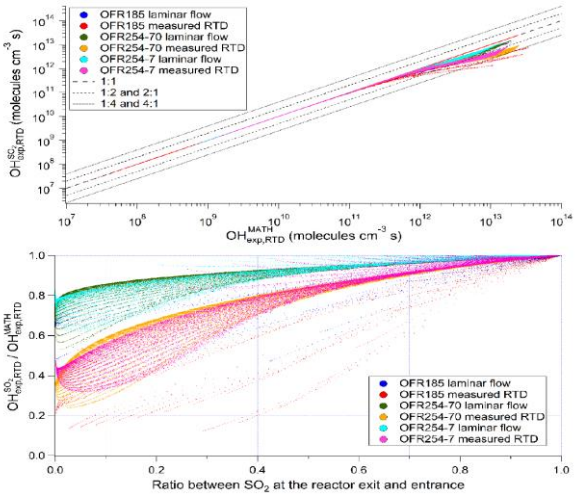

Figure 13. *(upper) OH exposures estimated from SO_2 decay in the models with residence time distributions ($OH_{exp,RTD}^{SO_2}$) vs. those calculated from direct integration for the models with residence time distributions ($OH_{exp,RTD}^{MATH}$). The 1:1, 1:2, 2:1, 1:4 and 4:1 lines are also shown for comparison. (lower) Ratios between the two types of OH exposures as a function of the fractional consumption of SO_2 in the reactor. The two methods give similar results under most conditions, but the SO_2 decay method tends to underestimate the true average OH_{exp} at highest exposures and lower fraction SO_2 remaining.*

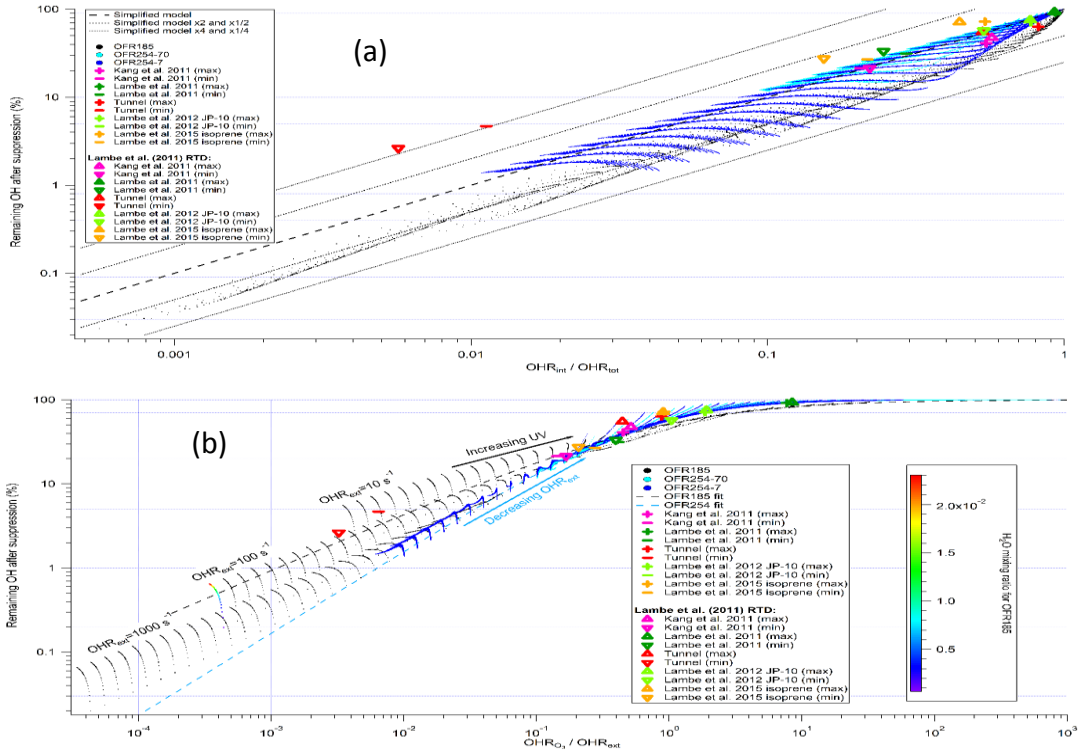

Figure 14. *Fraction of OH remaining after suppression by external OH reactivity (OHR_{ext}) vs (top) the ratios of internal reactivity to total OHR or (bottom) O_3 reactivity to OHR_{ext}. Small dots are for conditions run for the model in this study and symbols are for experimental studies where typically the effects were not (or only partially) accounted for. It is clear that under many conditions, failing to account for OH suppression (i.e. using calibrations where OHR_{ext} was absent) can lead to large underestimates in OH_{exp}.*

We also report two equations for estimating OH exposure in OFR254. We find that the equation estimating OH_{exp} from measured O_3 consumption performs better than an alternative equation that does not use it, and thus recommend measuring both input and output O_3 concentrations in OFR254 experiments. This study contributes to establishing a firm and systematic understanding of the gas-phase HO_x and O_x chemistry in these reactors, and enables better experiment planning and interpretation as well as improved design of future reactors.

Further details of this work can be found in Peng et al. (2015a).

2.1.3 Modeling Non-OH Chemistry in OFR185 and OFR254

Although use of OFRs using low-pressure Hg lamp emission at 185 and 254 nm produce OH radicals are widely used in atmospheric chemistry and other fields, knowledge of detailed OFR chemistry is limited. In turn this knowledge gap has led to speculation in the literature about whether some non-OH reactants, including several not relevant for tropospheric chemistry, may play an important role in these OFRs. These non-OH reactants are UV radiation, O(1D), O(3P), and O_3. Therefore, we investigated the relative importance of other reactants to OH for the fate of reactant species in OFR under a wide range of conditions via box modeling. The relative importance of non-OH species is less sensitive to UV light intensity than to relative humidity (RH) and external OH reactivity (OHR_{ext}), as both non-OH reactants and OH scale roughly proportional to UV intensity. We show that for field studies in forested regions and also the urban area of Los Angeles, reactants of atmospheric interest are predominantly consumed by OH (*Figs. 15-17***)**. We find that O(1D), O(3P), and O_3 have relative contributions to VOC consumption that are similar or lower than in the troposphere (*Fig. 15*). The impact of O atoms can be neglected under most conditions in both OFRs and the troposphere. Under "pathological OFR conditions" of low RH and/or high OHR_{ext}, the importance of non-OH reactants is enhanced because OH is suppressed (*Figs. 15, 16*). Some biogenics can have substantial destructions by O_3 (*Fig. 17*), and photolysis at non-tropospheric wavelengths (185 and 254 nm) may also play a significant role in the degradation of some aromatics under pathological conditions (*Figs. 15, 16*). Working under low O_2 (and sufficient H_2O) with the OFR185 mode allows OH to completely dominate over O_3 reactions even for the biogenic species most reactive with O_3. Non-tropospheric VOC photolysis may have been a problem in some laboratory and source studies, but can be avoided or lessened in future studies by diluting source emissions and working at lower precursor concentrations in lab studies, and by humidification. SOA photolysis is shown to be insignificant for most functional groups, except for nitrates and especially aromatics, which may be photolyzed at high UV flux settings (*Fig. 18*). This modeling work further establishes the OFR's usefulness as a tool to study atmospheric chemistry and enables better experiment design and interpretation, as well as improved future reactor design.

Further details of this work can be found in Peng et al. (2015b).

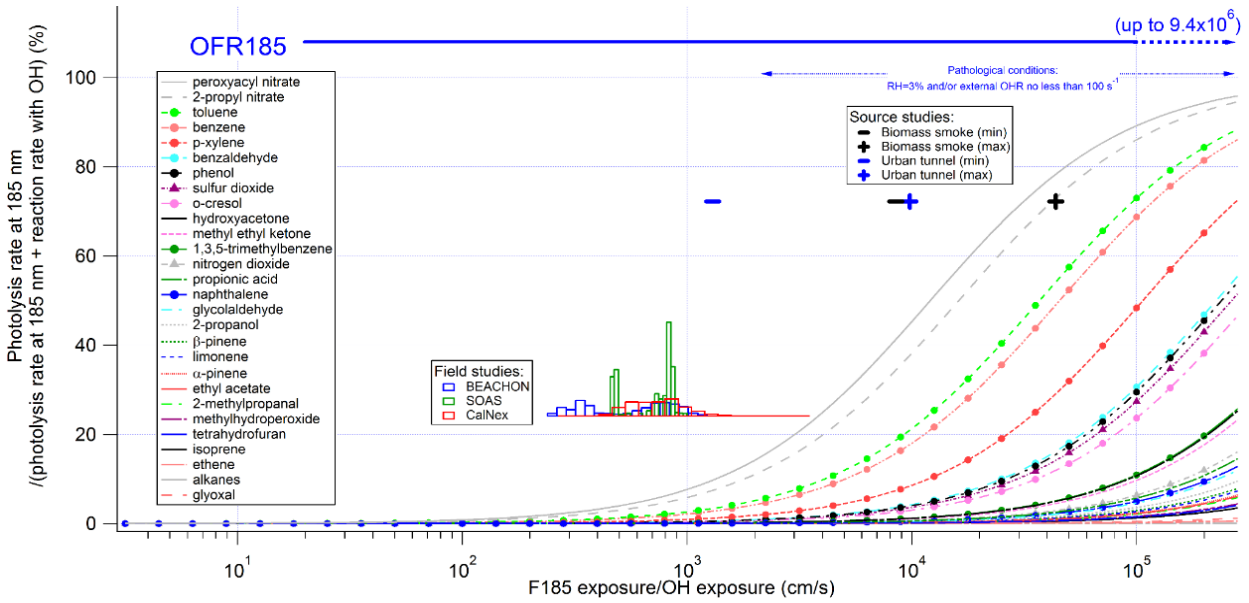

Figure 15. *Fractional importance of the photolysis rate at 185 nm of several species of interest vs. the reaction rate with OH, as a function of the ratio of exposure to 185 nm photons (F185) and OH. The modeled range for OFR185 and for "pathological conditions" for OFR185 are also shown. The curves of aromatics and inorganic gases are highlighted by solid dots and upward triangles, respectively. The lower inset shows histograms of model-estimated F185/OH exposures for three field studies where OFR185 was used to process ambient air. The upper inset shows the same information for source studies of biomass smoke (FLAME-3; (Ortega et al., 2013)) and an urban tunnel (Tkacik et al., 2014).*

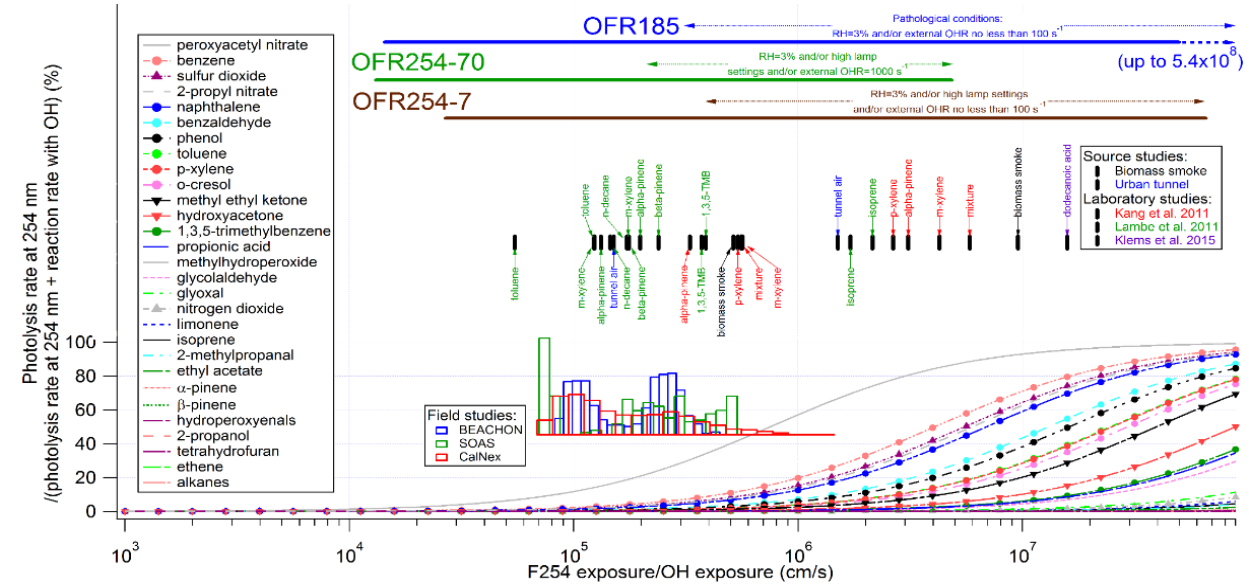

Figure 16. *Same format as Fig. 15, but for 254 nm photolysis. The modeled range for OFR254-70 and OFR254-7 and for corresponding pathological conditions are also shown. The insets show histograms of model-estimated F254/OH exposures for three field studies where OFR185 was used to process ambient air. In addition to source studies of biomass smoke (FLAME-3) and urban tunnel (Tkacik et al., 2014), F254 exposure/OH exposure ratios in two laboratory studies (Kang et al., 2011; Lambe et al., 2011b) are shown in the upper inset (with corresponding colored). The lower/upper limits of F254 exposure/OH exposure ratios in the experiments with a certain source in a certain study are denoted by tags below/above the markers, respectively. Curves of ketones are highlighted by downward triangles.*

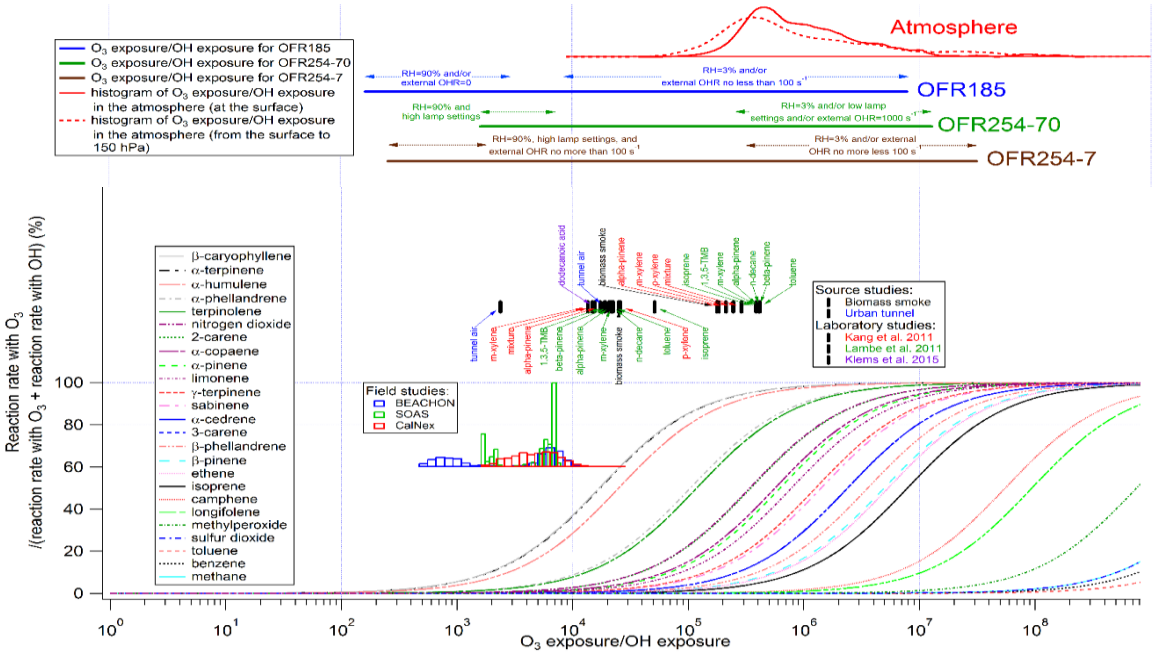

Figure 17. *Same format as Figs. 15/16, but for the fractional importance of the reaction rate with O_3 vs. OH as a function of the relative exposure of O_3 and OH. The curves of biogenics are highlighted by squares. Also shown are modeled distributions of the relative exposure of O_3 and OH at the Earth's surface (solid line) and throughout the column from the surface to a height with a pressure of 150 hPa (dashed line). The distributions were calculated from the mean daily concentrations of O_3 and OH as simulated by the GISS ModelE2.*

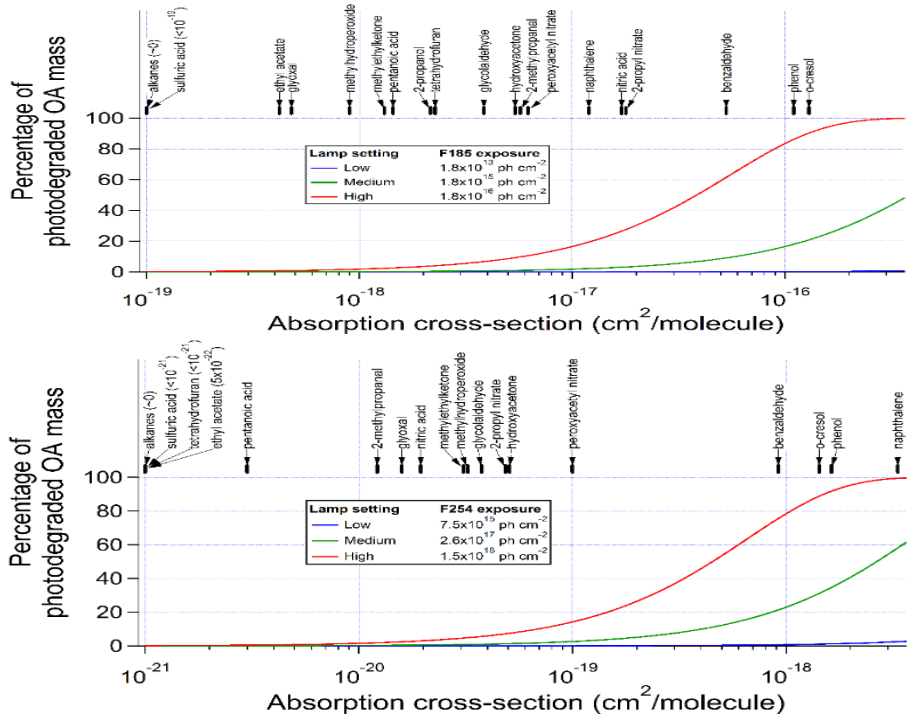

Figure 18. *Percentage of SOA photodegradation at (upper) 185 and (lower) 254 nm at different UV levels as a function of absorption cross-section under the assumption of unity quantum yield. Absorption cross-sections of some representative SOA components are also shown.*

2.2 Laboratory Studies of SOA Formation in Oxidation Flow Reactors

2.2.1 Secondary Organic Aerosol Yields from VOC standards

In the laboratory, we conducted a series of aerosol yield studies and composition using different VOC reactants representative of important anthropogenic and biogenic SOA sources. These experiments included combustion byproducts (toluene, methyl naphthalene), terpenes (alpha-pinene, beta-pinene, 3-carene), sesqueterpines (longifolene), and methyl butenol (MBO). During these experiments, SOA yields and chemical composition were determined using AMS and SMPS and initial and consumed VOC reactants were measured by PTR-MS. Our results indicate that SOA yields in the OFR are similar to those reported for large environmental chambers, bolstering the case that OFRs can be used to quantitatively simulate atmospheric processes and that it can be used as a "transfer tool" between laboratory and field applications (for which large environmental chamber are less practical since they are less portable, much slower, and have much more limited aging capacity). Also, as we have observed in the atmosphere, laboratory results show similar characteristic aging extents where the destruction (fragmentation, evaporation) of SOA appears to overtake formation as observed by a net decrease in SOA production. Unlike environmental chambers that typically can only conduct experiments that simulate up to 1/2 to 2 days equivalent atmospheric processing and require several hours to complete, with the OFR we age samples for up to several weeks of atmospheric equivalent aging at a range of oxidant exposures every hour. Thus, during these experiments, it has been possible to explore the complex relationship of SOA yields to both existing organic aerosol mass and also at a large range of oxidant exposures. This ability is helping to interpret field OFR measurements where we have scanned a large range in oxidant exposure and in comparing measured vs modeled SOA.

2.2.2 Secondary Organic Aerosol from Crude Oil

We conducted laboratory studies of SOA formation from crude oil to help interpret SOA formation observed during aircraft studies conducted over the Gulf of Mexico during the 2010 Deep Water Horizon oil spill in collaboration with Dr. Joost de Gouw's group at NOAA. Crude oil was exposed to a continuous clean air stream resulting in evaporation and gradual distillation as more volatile compounds are removed. The evaporated VOCs were photochemically processed in the OFR and compounds spanning a broad range of volatilities (3-16 carbons) were quantified before and after the reactor and the resulting aerosol volume, mass and chemical composition were quantified with an SMPS and AMS. The time dependence of the evaporation as a function of volatility classes and the amount of each class reacted in the chamber were determined using VOC measurements (PTR-MS) (*Fig. 19*). Combining this information with the measurements of aerosol formation, multivariate linear regression fitting was used to calculate the time-dependent contributions of the different volatility classes of VOCs to SOA formation (*Fig. 20*). It was shown that intermediate volatility organic compounds (IVOCs; saturation vapor pressure, $C^*=10^5$-10^6 μg m^{-3}) contributes much more to SOA formation than the more volatile organic compounds ($C^* \geq 10^7$ μg m^{-3}; *Figs. 20, 21*), results consistent with analysis of the airborne measurements over the DWH oil spill (de Gouw et al., 2011). The chemical

composition of the aerosol produced was also similar to that observed over the spill (*Fig. 22*). Further details of this work can be found in Li et al. (2013).

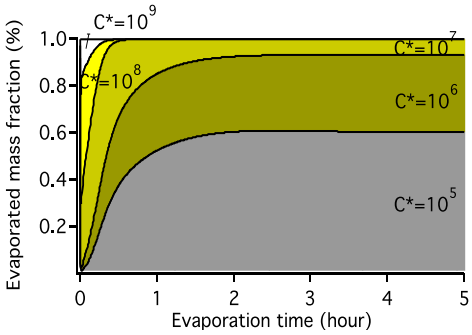

Figure 19. *Time series of relative mass fraction of evaporated hydrocarbon vapors without photooxidation for C*(10^5–10^9 μg m^{-3}).*

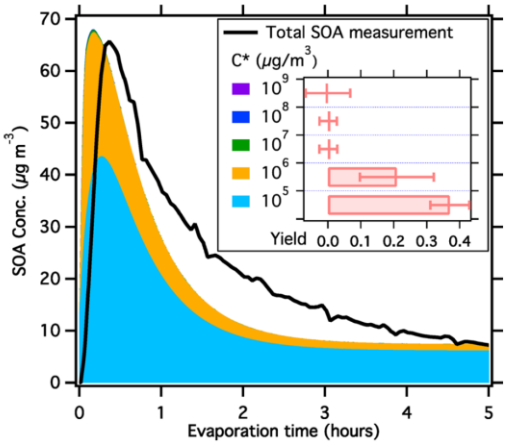

Figure 20. *Measured SOA concentration and fit of SOA contribution from each C* class. SOA yields shown in the inset were estimated from the multi-variate fitting. Compounds with C* =10^5–10^6 μg m^{-3} contribute most of the SOA mass.*

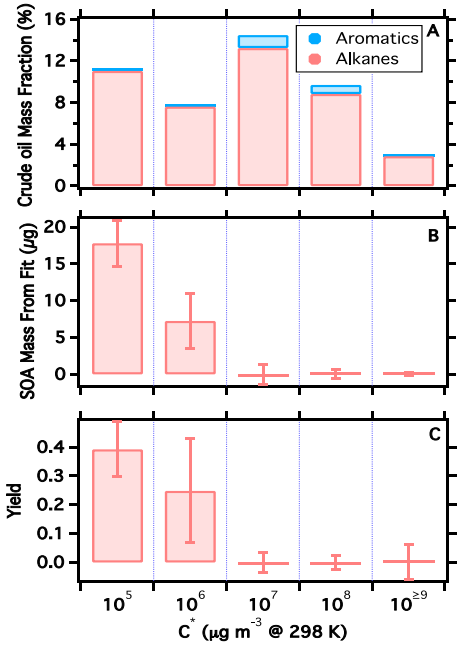

Figure 21. *Volatility distribution of (A) crude oil including measured aromatics and estimated alkanes (assuming the same composition as DWH oil spill), (B) Estimated SOA concentrations produced from compounds of each C* bin (C) Estimated SOA yields.*

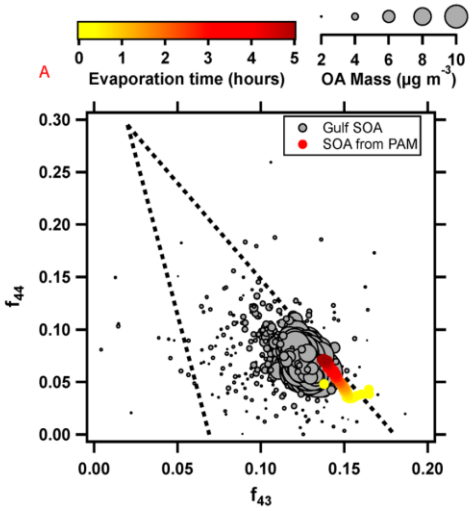

Figure 22. *Fractional contribution to total OA of ions at m/z 44 (f_{44}) vs. m/z 43 (f_{43}) in AMS spectra for Gulf SOA and laboratory data. The aerosol produced in the OFR has a similar mass spectrometric signature to SOA observed over the oil spill.*

2.2.3 MOVI-HRToF-CIMS – OFR

For the past five years, our group has been working on development of a Microorifice Volatilization Impactor High-Resolution Time-of-Flight Chemical-Ionization Mass Spectrometer (MOVI-HRToF-CIMS or with a newer version of inlet, FIGAERO-HRToF-CIMS) capable of detecting organic acids in both the particle and gas phases, quantitatively and with very high sensitivity. Using at prototype MOVI- HRToF-CIMS and OFR we acquired the first mass spectrum of SOA (α-pinene precursor) using this technique (*Fig. 23*). We observed high molecular weight ions representing oligomeric units present in much greater relative abundance in the particle phase. These results, obtained in near real-time, were remarkably similar to spectra obtained from offline analysis methods that require complicated sample handling and post analysis. This powerful new technique is proving to be another useful tool in understanding SOA formation in OFRs (and the atmosphere) at a mechanistic level.

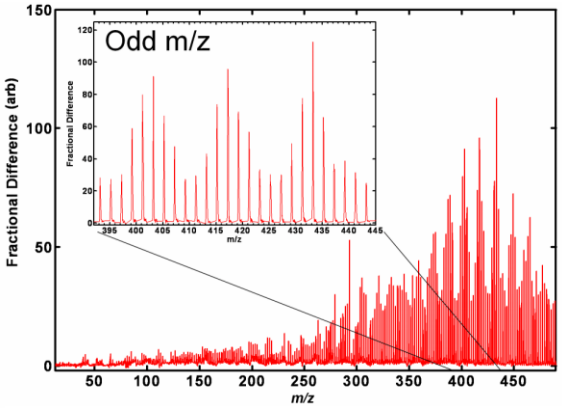

Figure 23. *Mass spectrum of OFR-generated α-pinene SOA desorbed from the MOVI impactor at ~130 °C. These real-time data, which demonstrate the ability of the MOVI- HRToF-CIMS to detect high molecular weight oligomeric units, are similar to published data using offline techniques.*

3. Applications of Laboratory and Modeling Studies to Field Measurements using OFRs and Modeling SOA Formation.

The main motivation for conducting the series laboratory and modeling studies of gas-phase oxidation and SOA formation in the OFR (described above) was to provide the understanding and tools to better interpret OFR field measurements of SOA formation and aging. In this section we show examples of how some of the results have been utilized as well as further modeling efforts aimed at quantitatively investigating SOA formation and OA aging for ambient air with OFR. The information is presented as figures with descriptive captions summarizing the main aspects and relevance.

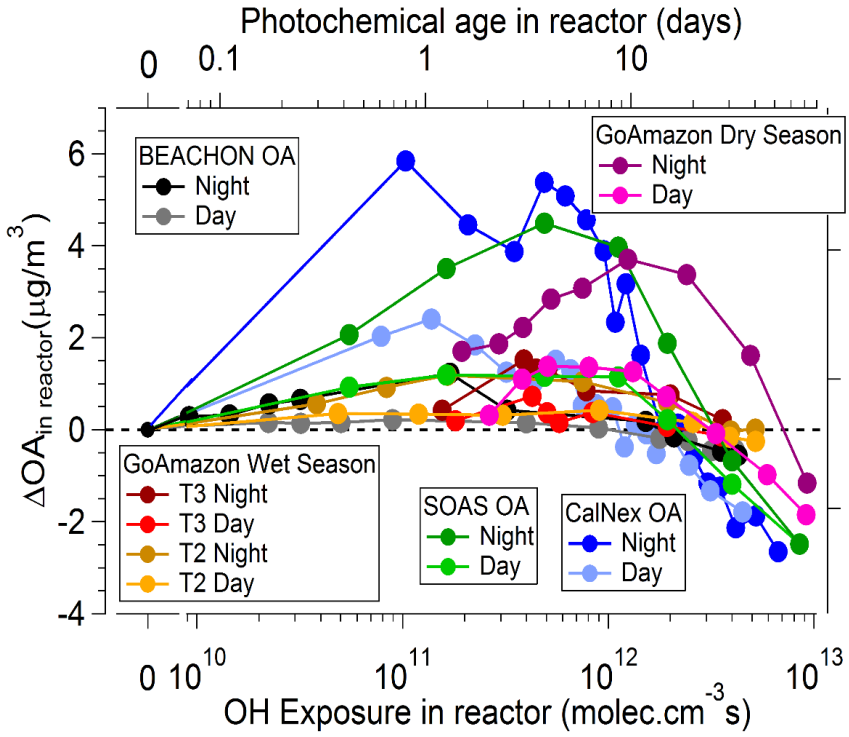

Figure 24. OA enhancements (compared to ambient OA) as a function of OH exposure in the OFR for several field campaigns separated by day/night: CalNeX-LA (urban, (Ortega et al., 2015)), BEACHON-RoMBAS (montane Colorado conifer forest, (Palm et al., 2015)), SOAS (mixed forest, semi-polluted SE US, (Hu et al., 2016b)), and GoAmazon2014/15 (Amazonia, periodically polluted, 2 sites (Palm et al., 2016b)). SOA production peaks at 1-4 days atmospheric equivalent aging then decreases at higher ages shows net OA loss at highest ages (>5-20 days). This show the shifting balance between functionalization and condensation at lower ages to fragmentation and evaporation at higher ages. Although the behavior is qualitatively similar for the different measurements, the OH_{exp} ranges where the different processes appear to dominate are different, an observation that is only possible and accurate with the advanced understanding of quantifying OH_{exp} gained through the modeling and laboratory work that was conducted. In practice for the field campaigns, the OH_{exp} calibration equations we've developed are used in combination with any tracers species decay measurements to determine the most accurate and high-data coverage calculations of OH_{exp} (Palm et al., 2015).

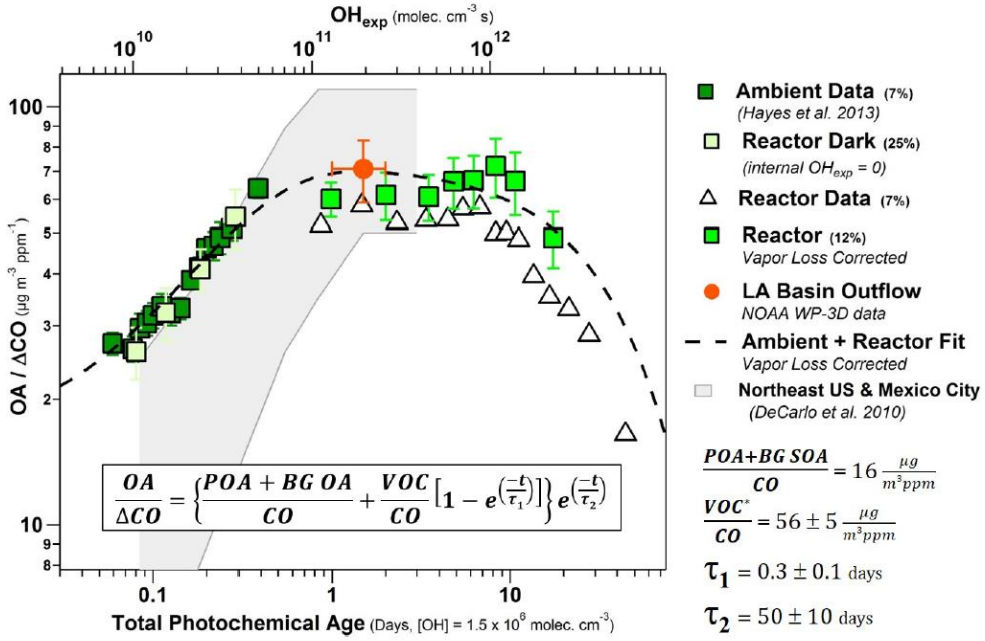

Figure 25. Ratio of OA to excess carbon monoxide (above background levels) vs. total photochemical age in days for ambient and reactor data during CalNex-LA (Pasadena, CA). Also shown in the value for LA-Basin outflow from aircraft measurements from the NOAA WP-3D during CalNex (Bahreini et al., 2012). Averages for quantiles of ambient (7%), reactor (7%), reactor dark (25%, internal OH_{exp} = 0) and reactor vapor loss-corrected (12%; see *Fig. 29*) data are shown. A fit to reactor data is also shown. Results from field studies in the NE US and Mexico City are shown in the background (DeCarlo et al., 2010). This provides another example of the quantitative information on SOA formation and OA aging for ambient air possible using the OFR that relies on accurate OH_{exp} determination. (Ortega et al., 2015)

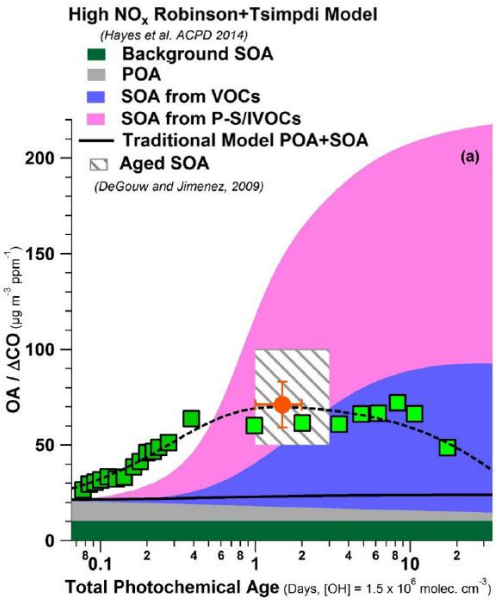

Figure 26. Comparison of OFR data with model results for evolution of OA/ΔCO vs. total photochemical age with traditional SOA formation model, high NO_x Robinson+Tsimpidi model from Hayes et al. (2015). Also shown is the summary of urban aged ratios from de Gouw and Jimenez (2009). Such observational vs modeling comparisons are important to testing and constraining modeling studies and in this case shows the large underestimation of SOA production for traditional SOA models and possibly overproduction of more updated models at higher ages. Comparison at the higher ages was only possible by use of the OFR to reach much higher aging that observed in ambient air. (Ortega et al., 2015)

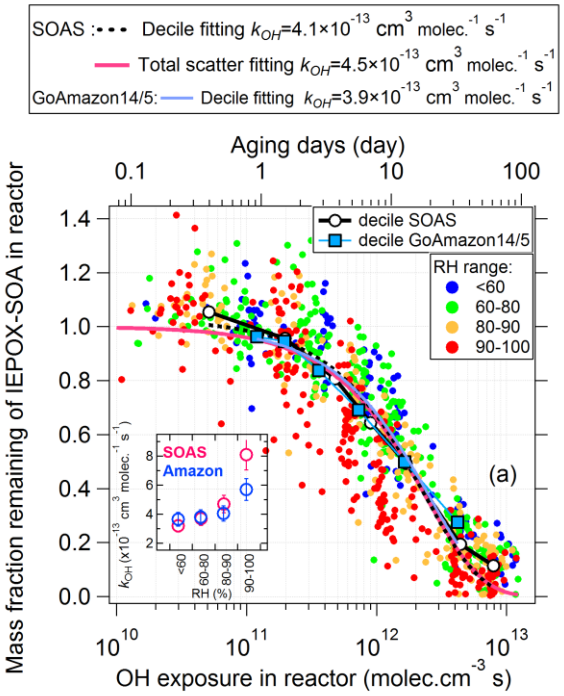

Figure 27. Mass fraction remaining of IEPOX-SOA as a function of OH_{exp} in the OFR during the SOAS and GoAmazon2014/15 (dry season) campaigns. The inset shows the RH-dependent calculated k_{OH} for both studies. Individual data points from SOAS are color-coded by ambient RH. IEPOX-SOA, SOA formed through reactive uptake of IEPOX gas (formed through low-NO_x oxidation of isoprene) onto particles, was separated from the bulk OA in the outflow of the OFR using Positive Matrix Factorization (PMF). The high exposures accessible with OFR, combined with accurately-determined OH_{exp}, allowed for quantitative determination of the heterogeneous OH oxidation loss rate of IEPOX-SOA and thus an estimate of the lifetime in the atmosphere due to this loss process. (Hu et al., 2016a)

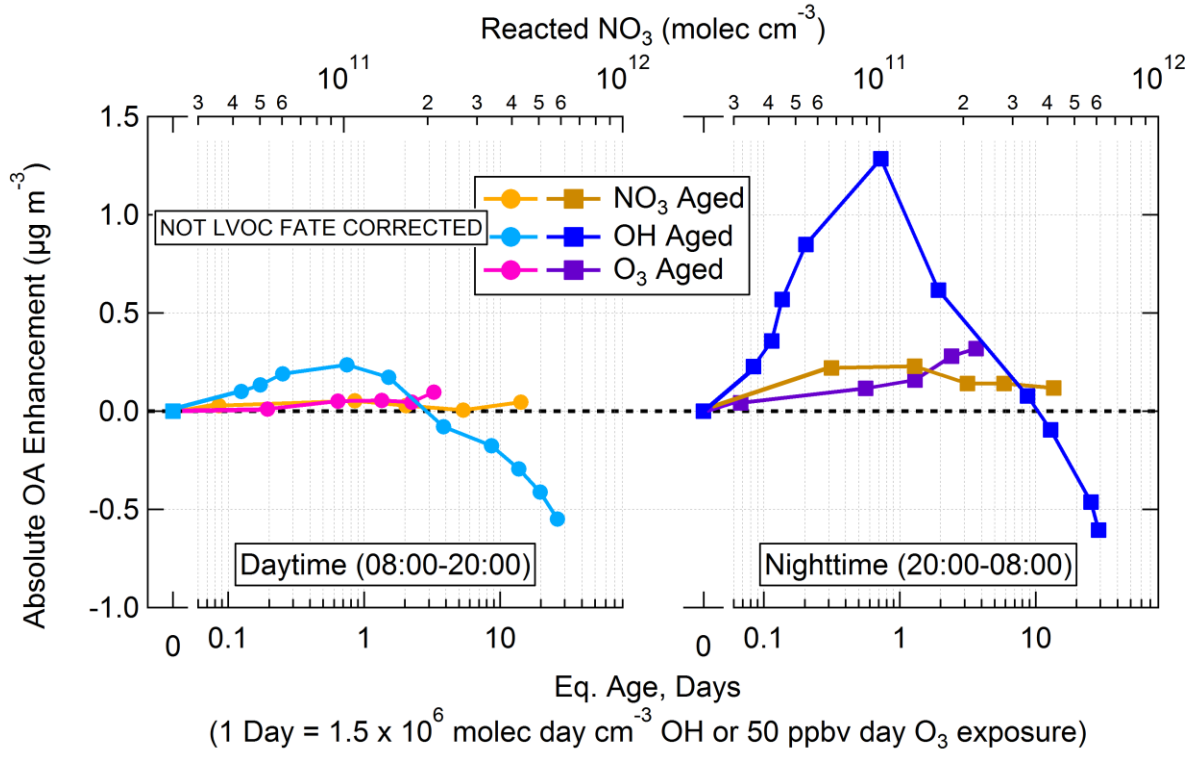

Figure 28. OA enhancement vs. age for OH, O_3, and NO_3 oxidation, separated into daytime and nighttime data for the BEACHON-RoMBAS campaign (montane Colorado coniferous forest). OH oxidation produced several times more OA enhancement than O_3 and NO_3 oxidation, and loss of OA due to heterogeneous oxidation was only observed for OH oxidation for the ages explored. (Palm et al., 2016a)

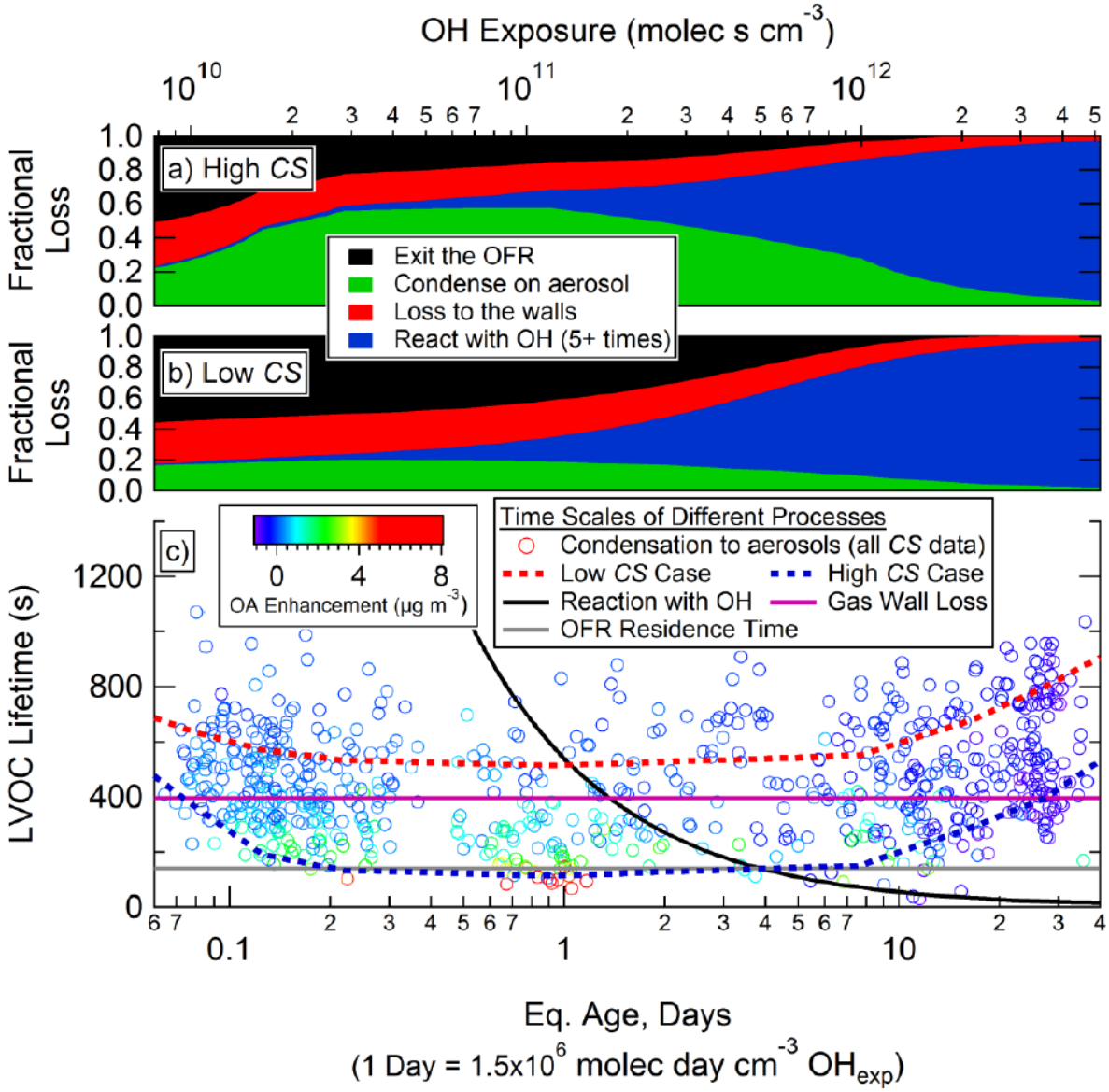

Figure 29. Modeled fractional fates of loss of low-volatility organic compounds (LVOCs) to OFR walls, condensation to aerosols, reaction with OH to produce volatile products, or exiting the OFR to be lost on sampling line walls as a function of photochemical age for **(a)** high condensational sink (CS) and **(b)** low CS cases; **(c)** LVOC lifetimes for each of these pathways (BEACHON-RoMBAS campaign). Lifetime for condensation to aerosols is shown for all data points (colored by OA enhancement after oxidation) using CS calculated from SMPS measurements. While in the atmosphere nearly 100% of LVOCs would condense on aerosols, in the OH-OFR for conditions at BEACHON, >20-70% condense at OH_{exp} where maximum OA enhancement occurs. Limitations are due to the short timescale of the reactor (~3 min) and modest aerosol surface area. This model was developed to better understand the fate of functionalized compounds formed by OH oxidation within the OFR and quantify and correct for pathways that would reduce observed SOA formation in the OFR and not be present in the ambient atmosphere. The details of this model are described in detail in Palm et al. (2015) and examples of its application are shown in *Figs. 30, 31*.

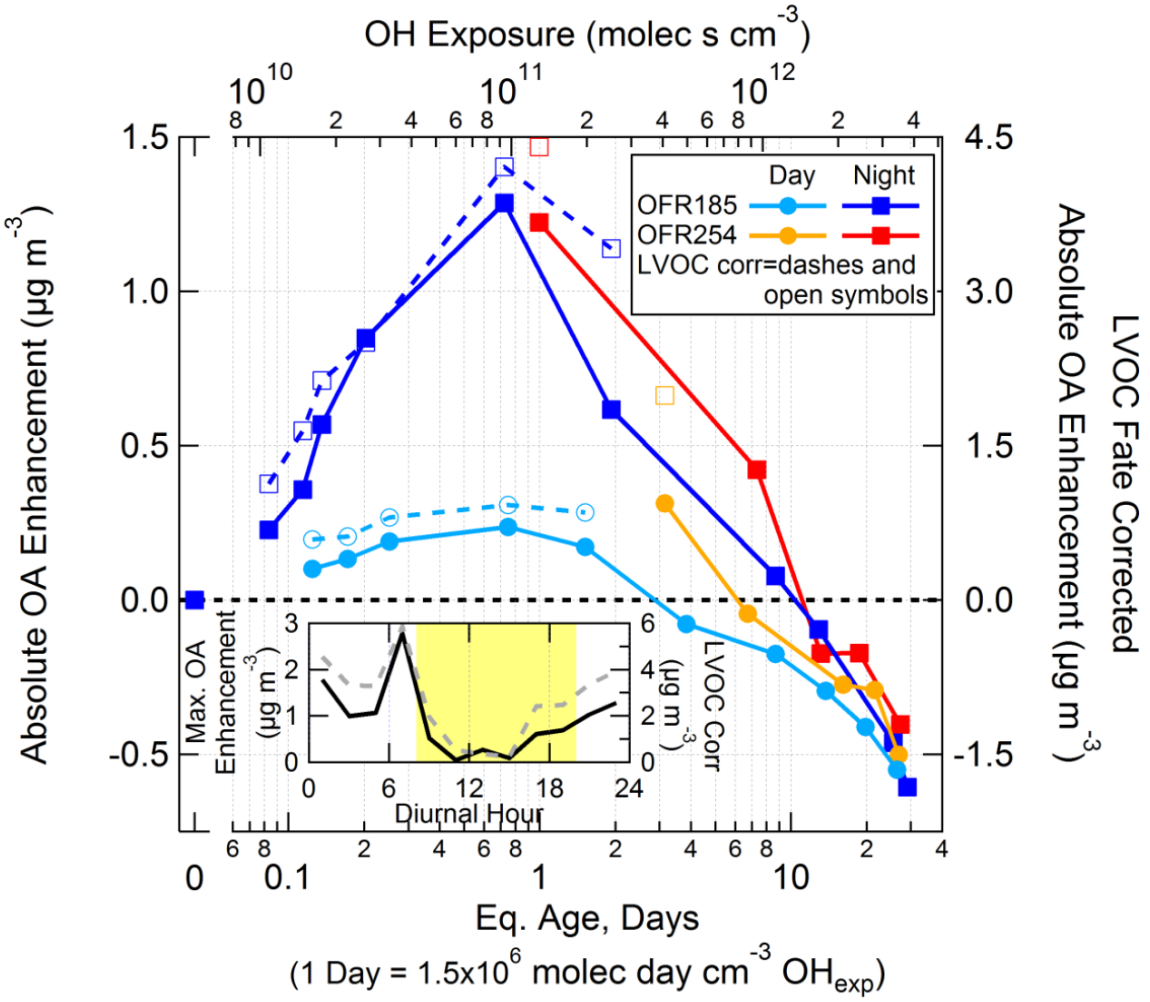

Figure 30. Comparison of absolute OA enhancement from OH oxidation using the OFR185 and OFR254 methods (BEACHON-RoMBAS campaign), binned by photochemical age and separated into daytime (08:00–20:00 LT) and nighttime (20:00–08:00 LT) to reflect the changes in ambient SOA precursors between day and night. OH_{exp} was calculated using the calibration equations we developed in Li et al. (2015) and Peng et al. (2015a) in combination with in-situ tracer decay measurements. Data are shown with (right axis, open symbols, and dashed lines) and without (left axis, closed symbols and solid lines) the LVOC fate correction described in *Fig. 29*. Inset: the maximum OA enhancement (all data 0.4–1.5 days eq. age) as a function of time of day, with (dashed) and without (solid) the LVOC fate correction. OFR254 measurements with positive OA enhancement were multiplied by the ratio of ambient MT concentrations measured during OFR185 vs. OFR254 sampling periods (ratio= 1.8). Negative OA enhancements were not normalized in this way since the amount of mass lost due to heterogeneous oxidation would not necessarily correlate with ambient MT concentrations. These results highlight the importance of applying condensation corrections to estimate atmospherically-relevant SOA production in ambient air with moderate-to-low aerosol loading and also the comparability of the OFR185 and OFR254 methods in terms of SOA mass production. (Palm et al., 2015)

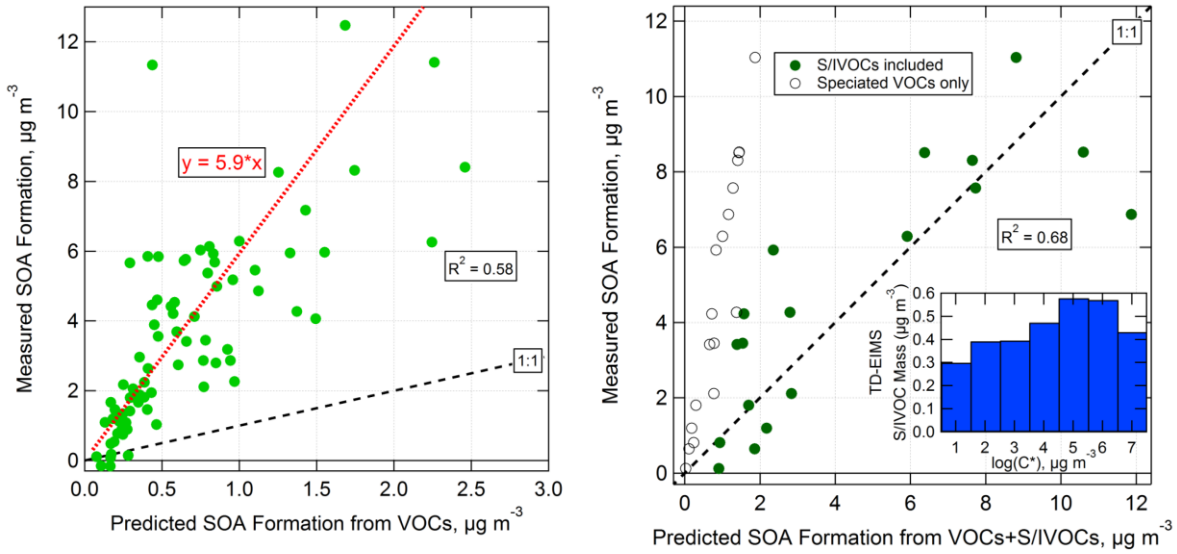

Figure 31 (left panel). Measured vs. predicted SOA formation from OH oxidation of ambient air in an OFR using the OFR185 method (BEACHON-RoMBAS campaign). Only the range of photochemical ages with the highest SOA formation (0.4–1.5 eq. days) was used, and the LVOC fate correction was applied (see *Fig. 29*). Predicted SOA formation was calculated by applying OA concentration-dependent yields (average of 13.3, 14.9, 15.9, and 1.8% for monoterpenes, sequiterpenes, toluene+*p*-cymene, and isoprene, respectively, with average OA concentration of 5.1 µgm^{-3}) to VOCs reacted in the OFR (Tsimpidi et al., 2010). The amount of reacted VOCs was estimated using OH_{exp} and ambient VOC concentrations. If a non-zero *y* intercept is allowed, the regression line becomes $y = 7.0x - 1.0$.

Figure 31 (right panel). Same data as shown in left panel except only including data when there was temporal overlap of measurements of volatility-separated semi/intermediate VOCs (S/IVOCS) using a novel TD-EIMS method (Cross et al., 2013; Hunter et al., 2016). Predicted SOA formation is estimated using VOCs (as in left panel) with (green filled circles) and without (open circles) including an empirical 80% SOA yield from S/IVOCs measured by the TD-EIMS (a lower limit of total S/IVOCs). Inset: average S/IVOC concentrations as a function of the log of the saturation vapor concentration, *C**.

The analysis shown in these figures (*Fig. 31 left/right*) demonstrates the synthesis of OFR measurements using OH_{exp} estimations, LVOC-fate / condensation modeling corrections, VOC – SOA yields and novel S/IVOC measurements to better understand and quantify in situ SOA formation potential in a biogenic-dominated forest region. The results suggest that for the ensemble of instantaneous snapshots of SOA formation potential in this environment, compounds other than traditionally-measured VOC account for most of the SOA formation, which likely are photochemically-produced oxidation products. (Palm et al., 2015)

4. FIGAERO/MOVI-HRToF-CIMS for Studying Speciated & Bulk Gas-Particle Partitioning

In collaboration with U. Washington and Aerodyne Research Inc., our group has pioneered the development and application of new tools capable of measuring the chemical composition, gas/particle partitioning and particle-phase volatility - the Filter Inlet for Gases and Aerosols High-Resolution Time-of-Flight Chemical-Ionization Mass Spectrometer (FIGAERO-HRToF-CIMS, hereafter FIGAERO-CIMS for short) and the MOVI (micro-orifice volatilization impactor) variant (Yatavelli et al., 2012; Lopez-Hilfiker et al., 2014). The technique allows simultaneous measurement of gas- and particle-phase compounds through use of an aerosol collector. Gases can be analyzed while aerosols are sampled by the aerosol collector, and aerosols are later thermally desorbed under a zero air or nitrogen atmosphere. Chemical ionization (CI), a soft ionization technique preserving the parent ion in most cases, is used, and when combined with a high-resolution ToF analyzer it allows determination of the elemental composition of the molecular ions. In addition, by using different CI reagent ions (e.g., CH_3COO^-, I^-, $H_3O^+ \bullet (H_2O)_n$, NO_3^-) different compound classes can be detected. Gas and particle composition are quantified with the same HRToF detector at frequencies <1 hr making it ideal for capturing diurnal timescale changes in the atmosphere or tracking SOA formation and evolution in chamber studies. Our group successfully deployed the MOVI-CIMS for the first time in the field during BEACHON-RoMBAS, a study of biogenic aerosol in a pine forest in the Colorado Rockies (Yatavelli et al., 2014), and also successfully deployed a FIGAERO-CIMS in the SOAS field study in 2013 (Thompson et al., 2015). In both deployments, acetate ($CH_3C(O)O^-$) was used as the reagent ion to selectively ionize acids. Using ambient BEACHON-RoMBAS data we have investigated gas/particle partitioning, as the fraction in particle phase (F_p), of C_1-C_{18} alkanoic acids, six ions having elemental compositions similar to known terpenoic acids, and total bulk organic acids. *Figure 32* shows measurements of the F_p of C_1-C_{18} alkanoic acids. With increasing carbon number (lower volatility), greater fractions were observed in the particle phase, the magnitude of which matched modeled partitioning within the range of published vapor pressures, indicating that, on a daily timescale, alkanoic acids were close to thermodynamic equilibrium with the gas phase and providing convincing evidence that the MOVI-CIMS is a useful tool for studying partitioning of semivolatile compounds in a complex environment.

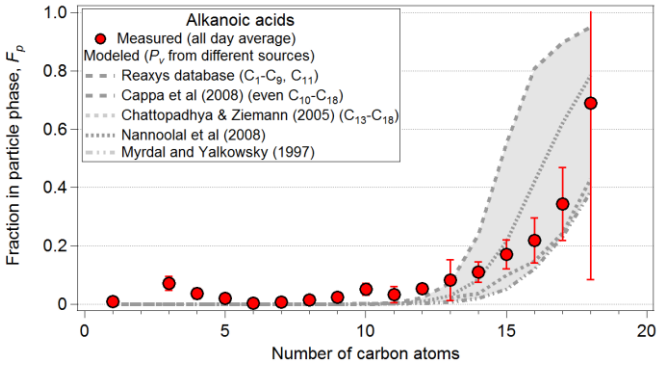

Figure 32. *Gas/particle partitioning as a function of carbon number for measured (●) and modeled (lines) alkanoic acids using different published $P°_{L,i}$ and ΔH_{vap} values (Yatavelli et al., 2014).*

Figure 33 shows the partitioning of the bulk (total) acids as a function of carbon number, *which to our knowledge was determined for the first time in that experiment.* Also shown is the "excess oxygen" (in addition to the known 2 oxygen atoms present in the organic acid functional group) as determined by the elemental analysis and mass quantification of each ion detected. The modeled partitioning assumes that the excess oxygen is contained in different organic functional groups (as indicated in *Fig. 33*). Carbon number and oxygen content were observed to be good predictors for partitioning, and the model assuming addition of an OH group to alkanoic acids (consistent with the conclusions of Ng et al. (2011) for the ambient evolution of SOA) reproduces the observed partitioning for C_7-C_{17}. While the more intermediate volatility species match the models relatively well, the lower volatility species tended to show higher apparent particle-phase fractions than the model predicted, suggesting possible adsorption or decomposition / fragmentation artifacts or that different isomeric compounds than those modeled may have been present.

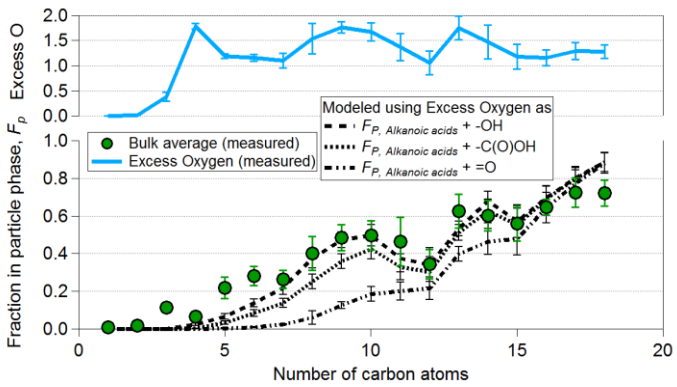

Figure 33. *Partitioning for bulk averaged acids binned into carbon number bins and modeled partitioning calculated using excess oxygen as different organic functional groups, for the average of the whole study (Yatavelli et al., 2014).*

Figure 34 shows the time series of observed and modeled partitioning for pinic acid, a well-known oxidation product of monoterpenes, from a study conducted in a terpene-dominated pine forest. The observed F_p is quite similar to the modeled values, and there are clear shifts in partitioning closely following ambient temperature (changes in total OA and particle water had only minor effects). Similar results were observed for other / bulk acids acids (Yatavelli et al., 2014), suggesting that they evaporate from the particle phase to re-establish gas-particle equilibrium on short timescales of < 1-2 hrs, and thus partitioning appears to not be effected by large kinetic limitation as has been suggested for some conditions and chemical systems in several recent studies that use less direct and non-

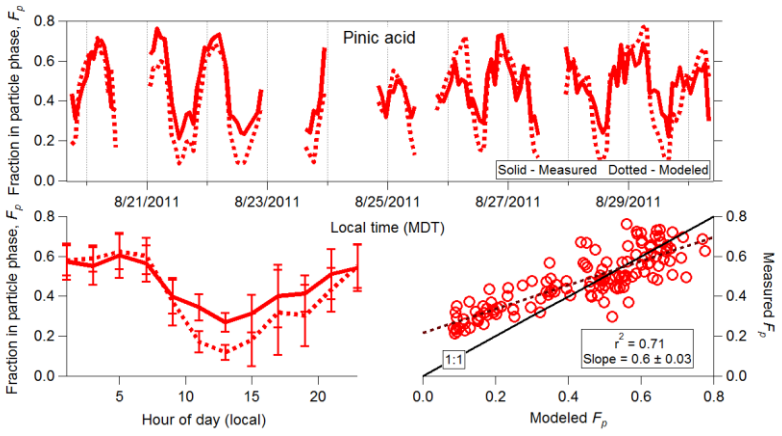

Figure 34. *Measured and modeled partitioning of pinic acid determined with the MOVI-HRToF-CIMS during the BEACHON-RoMBAS field study (Yatavelli et al., 2014).*

chemically-speciated methods (e.g., Virtanen et al., 2010; Vaden et al., 2011; Perraud et al., 2012; Renbaum-Wolff et al., 2013).

5. ASR/ARM Program Meeting Participation

Our group participated in and presented results at all of the ASR/ARM Program meetings (Fall Working Group Meetings, Spring PI Science Meetings) over the duration of this grant period. This has included oral presentations on the GVAX recon/planning trip, OFR results and gas-particle partitioning results at the Fall Working Group Meetings; poster presentations at the Spring PI Science Meetings (on OFR and partitioning); and co-organization of a break-out group on secondary organic aerosol at a FWGM.

Conclusions

The research conducted under this grant was highly successful. A wide range of topics were explored that focused on understanding the radical chemistry of oxidation flow reactors (OFRs) and applications of OFRs for investigating secondary organic aerosol (SOA) formation and OA aging. A gas-phase photochemical model was developed and was central to understanding and quantifying the radical chemistry in OFRs and then applying those results to better interpret laboratory and field applications of OFR. This work will have important impacts on the study of SOA formation on OA aging by providing a clear framework for designing and interpreting OFR studies in the lab and field. OFRs have recently become increasingly common for studying gas and aerosols chemistry of the atmosphere, and prior to this work, the lack of understanding of the basic chemistry and functionality of OFRs had a strong potential to result in poorly-designed experiments, inaccurate quantification, and speculation of weaknesses of the use of OFRs that lacked a sound basis. Much of results from the research conducted here has already been applied to several of our field and source studies, greatly improving the accuracy and ability to precisely interpret the scientific results. Improved knowledge of the formation of SOA and aging of OA is a critical component of better understanding aerosol life cycle in the atmosphere. This work demonstrates that use of OFRs can play an important role in gaining this new insight, complementing ambient field measurements, modeling and chamber studies.

Acknowledgements

We gratefully acknowledge the DOE/ASR for their financial support that made this research possible (under contract No. DE-SC0006035).

References

Aiken, A. C., Decarlo, P. F., Kroll, J. H., Worsnop, D. R., Huffman, J. A., Docherty, K. S., Ulbrich, I. M., Mohr, C., Kimmel, J. R., Sueper, D., Sun, Y., Zhang, Q., Trimborn, A., Northway, M., Ziemann, P. J., Canagaratna, M. R., Onasch, T. B., Alfarra, M. R., Prevot, A. S. H., Dommen, J., Duplissy, J., Metzger, A., Baltensperger, U. and Jimenez, J. L.: O/C and OM/OC ratios of primary, secondary, and ambient organic aerosols with high-resolution time-of-flight aerosol mass spectrometry, Environ. Sci. Technol., 42(12), 4478–4485, 2008.

Bahreini, R., Middlebrook, a. M., de Gouw, J. a., Warneke, C., Trainer, M., Brock, C. a., Stark, H., Brown, S. S., Dube, W. P., Gilman, J. B., Hall, K., Holloway, J. S., Kuster, W. C., Perring, a. E., Prevot, a. S. H., Schwarz, J. P., Spackman, J. R., Szidat, S., Wagner, N. L., Weber, R. J., Zotter, P. and Parrish, D. D.: Gasoline emissions dominate over diesel in formation of secondary organic aerosol mass, Geophys. Res. Lett., 39(6), n/a–n/a, 2012.

Charlson, R. J., Schwartz, S. E., Hales, J. M., Cess, R. D., Coakley, J. A., Hansen, J. E. and Hofmann, D. J.: Climate Forcing By Anthropogenic Aerosols, Science (80-.)., 255(5043), 423–430 [online] Available from: <Go to ISI>://A1992HA59000029, 1992.

Cross, E. S., Hunter, J. F., Carrasquillo, A. J., Franklin, J. P., Herndon, S. C., Jayne, J. T., Worsnop, D. R., Miake-Lye, R. C. and Kroll, J. H.: Online measurements of the emissions of intermediate-volatility and semi-volatile organic compounds from aircraft, Atmos. Chem. Phys., 13(15), 7845–7858, 2013.

DeCarlo, P. F., Ulbrich, I. M., Crounse, J., de Foy, B., Dunlea, E. J., Aiken, a. C., Knapp, D., Weinheimer, A. J., Campos, T., Wennberg, P. O. and Jimenez, J. L.: Investigation of the sources and processing of organic aerosol over the Central Mexican Plateau from aircraft measurements during MILAGRO, Atmos. Chem. Phys., 10(12), 5257–5280, 2010.

Dzepina, K., Volkamer, R. M. R., Madronich, S., Tulet, P., Ulbrich, I. M., Zhang, Q., Cappa, C. D., Ziemann, P. J. and Jimenez, J. L.: Evaluation of recently-proposed secondary organic aerosol models for a case study in Mexico City, Atmos. Chem. Phys., 9(15), 5681–5709, 2009.

Ervens, B., Turpin, B. J. and Weber, R. J.: Secondary organic aerosol formation in cloud droplets and aqueous particles (aqSOA): a review of laboratory, field and model studies, Atmos. Chem. Phys., 11(21), 11069–11102, 2011.

de Gouw, J. A.: Budget of organic carbon in a polluted atmosphere: Results from the New England Air Quality Study in 2002, J. Geophys. Res., 110(D16), D16305, 2005.

de Gouw, J. A., Middlebrook, A. M., Warneke, C., Ahmadov, R., Atlas, E. L., Bahreini, R., Blake, D. R., Brock, C. a, Brioude, J., Fahey, D. W., Fehsenfeld, F. C., Holloway, J. S., Le Henaff, M., Lueb, R. a, McKeen, S. a, Meagher, J. F., Murphy, D. M., Paris, C., Parrish, D. D., Perring, a E., Pollack, I. B., Ravishankara, a R., Robinson, a L., Ryerson, T. B., Schwarz, J. P., Spackman, J. R., Srinivasan, a and Watts, L. a: Organic aerosol formation downwind from the Deepwater Horizon oil spill., Science (80-.)., 331(6022), 1295–1299, 2011.

de Gouw, J. and Jimenez, J. L.: Organic Aerosols in the Earth's Atmosphere, Environ. Sci. Technol., 43(20), 7614–7618, 2009.

Hallquist, M., Wenger, J. C., Baltensperger, U., Rudich, Y., Simpson, D., Claeys, M., Dommen, J., Donahue, N. M., George, C., Goldstein, A. H., Hamilton, J. F., Herrmann, H., Hoffmann,

T., Iinuma, Y., Jang, M., Jenkin, M. E., Jimenez, J. L., Kiendler-Scharr, A., Maenhaut, W., McFiggans, G., Mentel, T. F., Monod, A., Prevot, A. S. H., Seinfeld, J. H., Surratt, J. D., Szmigielski, R. and Wildt, J.: The formation, properties and impact of secondary organic aerosol: current and emerging issues, Atmos. Chem. Phys., 9(14), 5155–5236, 2009.

Hansen, J., Sato, M. and Ruedy, R.: Radiative forcing and climate response, J. Geophys. Res., 102(D6), 6831–6864, 1997.

Hayes, P. L., Carlton, A. G., Baker, K. R., Ahmadov, R., Washenfelder, R. a., Alvarez, S., Rappenglück, B., Gilman, J. B., Kuster, W. C., de Gouw, J. a., Zotter, P., Prévôt, a. S. H., Szidat, S., Kleindienst, T. E., Offenberg, J. H., Jimenez, J. L., Ma, P. K. and Jimenez, J. L.: Modeling the formation and aging of secondary organic aerosols in Los Angeles during CalNex 2010, Atmos. Chem. Phys., 15(10), 5773–5801, 2015.

Heald, C. L., Jacob, D. J., Park, R. J., Russell, L. M., Huebert, B. J., Seinfeld, J. H., Liao, H. and Weber, R. J.: A large organic aerosol source in the free troposphere missing from current models, Geophys. Res. Lett., 32(18), L18809, 2005.

Hodzic, a., Aumont, B., Knote, C., Lee-Taylor, J., Madronich, S. and Tyndall, G.: Volatility dependence of Henry's law constants of condensable organics: Application to estimate depositional loss of secondary organic aerosols, Geophys. Res. Lett., 41(13), 4795–4804, 2014.

Hu, W., Palm, B. B., Day, D. A., Campuzano-Jost, P., Krechmer, J. E., de Sá, S. S., Martin, S. T., Alexander, M. L., Canonaco, F., Prevot, A. S. H., Brune, W. H. and Jimenez, J.-L.: The aging and low-volatility of Isoprene Epoxydiols-Derived Secondary Organic Aerosol (IEPOX-SOA) in real ambient environment: determination of reactive uptake coefficient (γ), in prep., 2016a.

Hu, W. W., Campuzano-Jost, P., Palm, B. B., Day, D. A. and Jimenez, J. L.: Measurements of Secondary Organic Aerosol Formation and OA Processing with an Oxidation Flow Reactor during the Southern Oxidant and Aerosol Study, In Prep., 2016b.

Hunter, J. F., Day, D. A., Yatavelli, R. N., Chan, A., Kaser, L., Cappellin, L., Hayes, P. L., Palm, B. B., Cross, E. B., Carrasquillo, A., Campuzano-Jost, P., Stark, H., Zhao, Y., Hohaus, T., Smith, J. N., Hansel, A., Karl, T., Goldstein, A. H., Guenther, A., Worsnop, D. R., Thornton, J. A., Heald, C. L., Jimenez, J. L. and Kroll, J. H.: Comprehensive characterization of atmospheric organic carbon at a forested site, submitted, 2016.

Jimenez, J. L., Canagaratna, M. R., Donahue, N. M., Prevot, a S. H., Zhang, Q., Kroll, J. H., DeCarlo, P. F., Allan, J. D., Coe, H., Ng, N. L., Aiken, a C., Docherty, K. S., Ulbrich, I. M., Grieshop, a P., Robinson, a L., Duplissy, J., Smith, J. D., Wilson, K. R., Lanz, V. A., Hueglin, C., Sun, Y. L., Tian, J., Laaksonen, A., Raatikainen, T., Rautiainen, J., Vaattovaara, P., Ehn, M., Kulmala, M., Tomlinson, J. M., Collins, D. R., Cubison, M. J., Dunlea, J., Huffman, J. a, Onasch, T. B., Alfarra, M. R., Williams, P. I., Bower, K., Kondo, Y., Schneider, J., Drewnick, F., Borrmann, S., Weimer, S., Demerjian, K., Salcedo, D., Cottrell, L., Griffin, R., Takami, a, Miyoshi, T., Hatakeyama, S., Shimono, a, Sun, J. Y., Zhang, Y. M., Dzepina, K., Kimmel, J. R., Sueper, D., Jayne, J. T., Herndon, S. C., Trimborn, a M., Williams, L. R., Wood, E. C., Middlebrook, A. M., Kolb, C. E., Baltensperger, U., Worsnop, D. R., Dunlea, E. J., Huffman, J. a, Onasch, T. B., Alfarra, M. R., Williams, P. I., Bower, K., Kondo, Y., Schneider, J., Drewnick, F., Borrmann, S., Weimer, S., Demerjian, K., Salcedo, D., Cottrell, L., Griffin, R., Takami, a, Miyoshi, T., Hatakeyama, S., Shimono, a, Sun, J. Y.,

Zhang, Y. M., Dzepina, K., Kimmel, J. R., Sueper, D., Jayne, J. T., Herndon, S. C., Trimborn, a M., Williams, L. R., Wood, E. C., Middlebrook, A. M., Kolb, C. E., Baltensperger, U. and Worsnop, D. R.: Evolution of organic aerosols in the atmosphere., Science (80-.)., 326(5959), 1525–9, 2009.

Kalberer, M., Paulsen, D., Sax, M., Steinbacher, M., Dommen, J., Prevot, a S. H., Fisseha, R., Weingartner, E., Frankevich, V., Zenobi, R. and Baltensperger, U.: Identification of polymers as major components of atmospheric organic aerosols., Science (80-.)., 303(5664), 1659–62, 2004.

Kanakidou, M., Seinfeld, J. H., Pandis, S. N., Barnes, I., Dentener, F. J., Facchini, M. C., Van Dingenen, R., Ervens, B., Nenes, A., Nielsen, C. J., Swietlicki, E., Putaud, J. P., Balkanski, Y., Fuzzi, S., Horth, J., Moortgat, G. K., Winterhalter, R., Myhre, C. E. L., Tsigaridis, K., Vignati, E., Stephanou, E. G. and Wilson, J.: Organic aerosol and global climate modelling: a review, Atmos. Chem. Phys., 5(4), 1053–1123, 2005.

Kang, E., Root, M. J., Toohey, D. W. and Brune, W. H.: Introducing the concept of Potential Aerosol Mass (PAM), Atmos. Chem. Phys., 7(22), 5727–5744, 2007.

Kang, E., Toohey, D. W. and Brune, W. H.: Dependence of SOA oxidation on organic aerosol mass concentration and OH exposure: experimental PAM chamber studies, Atmos. Chem. Phys., 11(4), 1837–1852, 2011.

Knote, C., Hodzic, A. and Jimenez, J. L.: The effect of dry and wet deposition of condensable vapors on secondary organic aerosols concentrations over the continental US, Atmos. Chem. Phys., 15(1), 1–18, 2015.

Kroll, J. H., Ng, N. L., Murphy, S. M., Varutbangkul, V., Flagan, R. C. and Seinfeld, J. H.: Chamber studies of secondary organic aerosol growth by reactive uptake of simple carbonyl compounds, J. Geophys. Res., 110(D23), D23207, 2005.

Lambe, A. T., Ahern, A. T., Williams, L. R., Slowik, J. G., Wong, J. P. S., Abbatt, J. P. D., Brune, W. H., Ng, N. L., Wright, J. P., Croasdale, D. R., Worsnop, D. R., Davidovits, P. and Onasch, T. B.: Characterization of aerosol photooxidation flow reactors: heterogeneous oxidation, secondary organic aerosol formation and cloud condensation nuclei activity measurements, Atmos. Meas. Tech., 4(3), 445–461, 2011a.

Lambe, A. T., Onasch, T. B., Massoli, P., Croasdale, D. R., Wright, J. P., Ahern, A. T., Williams, L. R., Worsnop, D. R., Brune, W. H. and Davidovits, P.: Laboratory studies of the chemical composition and cloud condensation nuclei (CCN) activity of secondary organic aerosol (SOA) and oxidized primary organic aerosol (OPOA), Atmos. Chem. Phys., 11(17), 8913–8928, 2011b.

Lambe, A. T., Chhabra, P. S., Onasch, T. B., Brune, W. H., Hunter, J. F., Kroll, J. H., Cummings, M. J., Brogan, J. F., Parmar, Y., Worsnop, D. R., Kolb, C. E. and Davidovits, P.: Effect of oxidant concentration, exposure time, and seed particles on secondary organic aerosol chemical composition and yield, Atmos. Chem. Phys., 15(6), 3063–3075, 2015.

Lane, T. E., Donahue, N. M. and Pandis, S. N.: Simulating secondary organic aerosol formation using the volatility basis-set approach in a chemical transport model, Atmos. Environ., 42(32), 7439–7451, 2008.

Li, R., Palm, B. B., Borbon, A., Graus, M., Warneke, C., Ortega, A. M., Day, D. a, Brune, W. H., Jimenez, J. L., de Gouw, J. a and Brune, B.: Laboratory studies on secondary organic aerosol

formation from crude oil vapors., Environ. Sci. Technol., 47(21), 12566–74, 2013.

Li, R., Palm, B. B., Ortega, A. M., Hlywiak, J., Hu, W., Peng, Z., Day, D. A., Knote, C., Brune, W. H., de Gouw, J. A. and Jimenez, J. L.: Modeling the radical chemistry in an oxidation flow reactor: radical formation and recycling, sensitivities, and the OH exposure estimation equation., J. Phys. Chem. A, 119(19), 4418–32, 2015.

Lim, Y. B., Tan, Y., Perri, M. J., Seitzinger, S. P. and Turpin, B. J.: Aqueous chemistry and its role in secondary organic aerosol (SOA) formation, Atmos. Chem. Phys., 10(21), 10521–10539, 2010.

Lopez-Hilfiker, F. D., Mohr, C., Ehn, M., Rubach, F., Kleist, E., Wildt, J., Mentel, T. F., Lutz, a., Hallquist, M., Worsnop, D. and Thornton, J. a.: A novel method for online analysis of gas and particle composition: Description and evaluation of a filter inlet for gases and AEROsols (FIGAERO), Atmos. Meas. Tech., 7(4), 983–1001, 2014.

Massoli, P., Lambe, a. T., Ahern, a. T., Williams, L. R., Ehn, M., Mikkilä, J., Canagaratna, M. R., Brune, W. H., Onasch, T. B., Jayne, J. T., Petäjä, T., Kulmala, M., Laaksonen, A., Kolb, C. E., Davidovits, P. and Worsnop, D. R.: Relationship between aerosol oxidation level and hygroscopic properties of laboratory generated secondary organic aerosol (SOA) particles, Geophys. Res. Lett., 37(24), n/a–n/a, 2010.

Myhre, G., Shindell, D., Bréon, F.-M., Collins, W., Fuglestvedt, J., Huang, J., Koch, D., Lamarque, J.-F., Lee, D., Mendoza, B., Nakajima, T., Robock, A., Stephens, G., Takemura, T. and Zhang, H.: Anthropogenic and Natural Radiative Forcing, in Climate Change 2013: The Physical Science Basis. Contribution of Working Group I to the Fifth Assessment Report of the Intergovernmental Panel on Climate Change, edited by T. F. Stocker, D. Qin, G.-K. Plattner, M. Tignor, S. K. Allen, J. Boschung, A. Nauels, Y. Xia, V. Bex, and P. M. Midgley, Cambridge University Press, Cambridge, United Kingdom and New York, NY, USA. [online] Available from: https://www.ipcc.ch/report/ar5/wg1/, 2013.

Ng, N. L., Canagaratna, M. R., Jimenez, J. L., Chhabra, P. S., Seinfeld, J. H. and Worsnop, D. R.: Changes in organic aerosol composition with aging inferred from aerosol mass spectra, Atmos. Chem. Phys., 11(13), 6465–6474, 2011.

Ortega, A. M., Day, D. A., Cubison, M. J., Brune, W. H., Bon, D., de Gouw, J. A. and Jimenez, J. L.: Secondary organic aerosol formation and primary organic aerosol oxidation from biomass burning smoke in a flow reactor during FLAME-3, Atmos. Chem. Phys., 13(22), 11551–11571, 2013.

Ortega, A. M., Hayes, P. L., Peng, Z., Palm, B. B., Hu, W., Day, D. A., Li, R., Cubison, M. J., Brune, W. H., Graus, M., Warneke, C., Gilman, J. B., Kuster, W. C., de Gouw, J. A. and Jimenez, J. L.: Real-time measurements of secondary organic aerosol formation and aging from ambient air in an oxidation flow reactor in the Los Angeles area, Atmos. Chem. Phys. Discuss., 15(15), 21907–21958, 2015.

Palm, B. B., Campuzano-Jost, P., Ortega, A. M., Day, D. A., Kaser, L., Jud, W., Karl, T., Hansel, A., Hunter, J. F., Cross, E. S., Kroll, J. H., Peng, Z., Brune, W. H. and Jimenez, J. L.: In situ secondary organic aerosol formation from ambient pine forest air using an oxidation flow reactor, Atmos. Chem. Phys. Discuss., 15(21), 30409–30471, 2015.

Palm, B. B., Campuzano-Jost, P., Ortega, A. M., Day, D. A., Karl, T., Kaser, L., Jud, W., Hansel, A., Fry, J. L., Brown, S. S., Zarzana, K. J., Dube, W. P., Wagner, N. L., Draper, D. C., Brune, W. H. and Jimenez, J. L.: Chemical properties of in-situ SOA formation using an oxidation

flow reactor in a pine forest, In prep., 2016a.

Palm, B. B., de Sá, S. S., Campuzano-Jost, P., Day, D. A., Hu, W. W., Seco, R., Park, J., Guenther, A., Kim, S., Brito, J., Wurm, F., Artaxo, P., Yee, L., Isaacman-VanWertz, G., Goldstein, A. H., Souza, R., Manzi, A. O., Vega, O., Tota, J., Newburn, M. K., Alexander, M. L., Martin, S. T., Brune, W. H. and Jimenez, J. L.: Measurements of in-situ SOA Formation Using an Oxidation Flow Reactor at GoAmazon2014/5, In prep., 2016b.

Peng, Z., Day, D. A., Stark, H., Li, R., Palm, B. B., Brune, W. H. and Jimenez, J. L.: HOx radical chemistry in oxidation flow reactors with low-pressure mercury lamps systematically examined by modeling, Atmos. Meas. Tech., 8, 4863–4890, 2015a.

Peng, Z., Day, D. A. A., Ortega, A. M. M., Palm, B. B. B., Hu, W. W., Stark, H., Li, R., Tsigaridis, K., Brune, W. H. H. and Jimenez, J. L.: Non-OH chemistry in oxidation flow reactors for the study of atmospheric chemistry systematically examined by modeling, Atmos. Chem. Phys. Discuss., 15(17), 23543–23586, 2015b.

Perraud, V., Bruns, E. a., Ezell, M. J., Johnson, S. N., Yu, Y., Alexander, M. L., Zelenyuk, A., Imre, D., Chang, W. L., Dabdub, D., Pankow, J. F. and Finlayson-Pitts, B. J.: Nonequilibrium atmospheric secondary organic aerosol formation and growth., Proc. Natl. Acad. Sci. U. S. A., 109(8), 2836–41, 2012.

Renbaum-Wolff, L., Grayson, J. W., Bateman, A. P., Kuwata, M., Sellier, M., Murray, B. J., Shilling, J. E., Martin, S. T. and Bertram, A. K.: Viscosity of α-pinene secondary organic material and implications for particle growth and reactivity., Proc. Natl. Acad. Sci. U. S. A., 110(20), 8014–9, 2013.

Spracklen, D. V., Jimenez, J. L., Carslaw, K. S., Worsnop, D. R., Evans, M. J., Mann, G. W., Zhang, Q., Canagaratna, M. R., Allan, J., Coe, H., McFiggans, G., Rap, a. and Forster, P.: Aerosol mass spectrometer constraint on the global secondary organic aerosol budget, Atmos. Chem. Phys., 11(23), 12109–12136, 2011.

Thompson, S. L., Yatavelli, R. L. N., Stark, H., Kimmel, J. R., Krechmer, J., Hu, W. W., Palm, B. P., Campuzano-Jost, P., Day, D. A., Isaacman, G., Goldstein, A. H., Khan, A., Holzinger, R., Lopez-Hilfiker, F., Mohr, C., Thornton, J. A., Jayne, J. T., Worsnop, D. R. and Jimenez, J. L.: Gas/particle partitioning of organic acids during the Southern Oxidant and Aerosol Study (SOAS): measurements and modeling, Submitt. to Aerosol Sci. Technol., 2015.

Tkacik, D. S., Lambe, A. T., Jathar, S., Li, X., Presto, A. a, Zhao, Y., Blake, D., Meinardi, S., Jayne, J. T., Croteau, P. L. and Robinson, A. L.: Secondary Organic Aerosol Formation from in-Use Motor Vehicle Emissions Using a Potential Aerosol Mass Reactor., Environ. Sci. Technol., 48(19), 11235–42, 2014.

Tsigaridis, K., Daskalakis, N., Kanakidou, M., Adams, P. J., Artaxo, P., Bahadur, R., Balkanski, Y., Bauer, S. E., Bellouin, N., Benedetti, A., Bergman, T., Berntsen, T. K., Beukes, J. P., Bian, H., Carslaw, K. S., Chin, M., Curci, G., Diehl, T., Easter, R. C., Ghan, S. J., Gong, S. L., Hodzic, A., Hoyle, C. R., Iversen, T., Jathar, S., Jimenez, J. L., Kaiser, J. W., Kirkevåg, A., Koch, D., Kokkola, H., Lee, Y. H., Lin, G., Liu, X., Luo, G., Ma, X., Mann, G. W., Mihalopoulos, N., Morcrette, J.-J., Müller, J.-F., Myhre, G., Myriokefalitakis, S., Ng, N. L., O'Donnell, D., Penner, J. E., Pozzoli, L., Pringle, K. J., Russell, L. M., Schulz, M., Sciare, J., Seland, Ø., Shindell, D. T., Sillman, S., Skeie, R. B., Spracklen, D., Stavrakou, T., Steenrod, S. D., Takemura, T., Tiitta, P., Tilmes, S., Tost, H., van Noije, T., van Zyl, P. G., von Salzen, K., Yu, F., Wang, Z., Wang, Z., Zaveri, R. a., Zhang, H., Zhang, K., Zhang, Q. and Zhang, X.:

The AeroCom evaluation and intercomparison of organic aerosol in global models, Atmos. Chem. Phys., 14(19), 10845–10895, 2014.

Tsimpidi, A. P., Karydis, V. A., Zavala, M., Lei, W., Molina, L., Ulbrich, I. M., Jimenez, J. L. and Pandis, S. N.: Evaluation of the volatility basis-set approach for the simulation of organic aerosol formation in the Mexico City metropolitan area, Atmos. Chem. Phys., 10(2), 525–546, 2010.

Vaden, T. D., Imre, D., Beranek, J., Shrivastava, M., Zelenyuk, A., Beránek, J., Shrivastava, M. and Zelenyuk, A.: Evaporation kinetics and phase of laboratory and ambient secondary organic aerosol., Proc. Natl. Acad. Sci. U. S. A., 108(6), 2190–5, 2011.

Virtanen, A., Joutsensaari, J., Koop, T., Kannosto, J., Yli-Pirilä, P., Leskinen, J., Mäkelä, J. M., Holopainen, J. K., Pöschl, U., Kulmala, M., Worsnop, D. R. and Laaksonen, A.: An amorphous solid state of biogenic secondary organic aerosol particles., Nature, 467(7317), 824–7, 2010.

Volkamer, R., Jimenez, J. L., San Martini, F., Dzepina, K., Zhang, Q., Salcedo, D., Molina, L. T., Worsnop, D. R. and Molina, M. J.: Secondary organic aerosol formation from anthropogenic air pollution: Rapid and higher than expected, Geophys. Res. Lett., 33(17), L17811, 2006.

Yatavelli, R. L. N., Lopez-Hilfiker, F., Wargo, J. D., Kimmel, J. R., Cubison, M. J., Bertram, T. H., Jimenez, J. L., Gonin, M., Worsnop, D. R. and Thornton, J. a.: A Chemical Ionization High-Resolution Time-of-Flight Mass Spectrometer Coupled to a Micro Orifice Volatilization Impactor (MOVI-HRToF-CIMS) for Analysis of Gas and Particle-Phase Organic Species, Aerosol Sci. Technol., 46(12), 1313–1327, 2012.

Yatavelli, R. L. N., Stark, H., Thompson, S. L., Kimmel, J. R., Cubison, M. J., Day, D. A., Campuzano-Jost, P., Palm, B. B., Hodzic, A., Thornton, J. a., Jayne, J. T., Worsnop, D. R. and Jimenez, J. L.: Semicontinuous measurements of gas–particle partitioning of organic acids in a ponderosa pine forest using a MOVI-HRToF-CIMS, Atmos. Chem. Phys., 14(3), 1527–1546, 2014.

Zhang, Q., Jimenez, J. L., Canagaratna, M. R., Allan, J. D., Coe, H., Ulbrich, I., Alfarra, M. R., Takami, A., Middlebrook, a. M., Sun, Y. L., Dzepina, K., Dunlea, E., Docherty, K., DeCarlo, P. F., Salcedo, D., Onasch, T., Jayne, J. T., Miyoshi, T., Shimono, A., Hatakeyama, S., Takegawa, N., Kondo, Y., Schneider, J., Drewnick, F., Borrmann, S., Weimer, S., Demerjian, K., Williams, P., Bower, K., Bahreini, R., Cottrell, L., Griffin, R. J., Rautiainen, J., Sun, J. Y., Zhang, Y. M. and Worsnop, D. R.: Ubiquity and dominance of oxygenated species in organic aerosols in anthropogenically-influenced Northern Hemisphere midlatitudes, Geophys. Res. Lett., 34(13), L13801, 2007.

Ziemann, P. J.: Evidence for low-volatility diacyl peroxides as a nucleating agent and major component of aerosol formed from reactions of O-3 with cyclohexene and homologous compounds, J. Phys. Chem. A, 106(17), 4390–4402, 2002.

Appendix 1: Publications Acknowledging this Grant

A total of 52 papers acknowledge this grant: 51 published and 1 under review. Numerous presentations at conferences have also acknowledged this grant (not listed, but can be provided upon request). These publications are listed below with bold indicating those led by our group (10).

Papers Published:

- Q. Zhang, J.L. Jimenez, M.R. Canagaratna, I.M. Ulbrich, S.N. Ng, D.R. Worsnop, and Y. Sun. Understanding Atmospheric Organic Aerosols via Factor Analysis of Aerosol Mass Spectrometry: a Review. *Analytical and Bioanalytical Chemistry*, 401, 3045-3067, DOI:10.1007/s00216-011-5355-y, 2011.
- **M.J. Cubison, A.M. Ortega, P.L. Hayes, D.K. Farmer, D.Day, M.J. Lechner, W.H. Brune, E. Apel, G.S. Diskin, J.A. Fisher, H.E. Fuelberg, A. Hecobian, D.J. Knapp, T. Mikoviny, D. Riemer, G.W. Sachse, W. Sessions, R.J. Weber, A.J. Weinheimer, A. Wisthaler, and J.L. Jimenez. Effects of Aging on Organic Aerosol from Open Biomass Burning Smoke in Aircraft and Laboratory Studies. *Atmospheric Chemistry and Physics*, 11, 12049-12064, doi:10.5194/acp-11-12049-2011, 2011.**
- **K.S. Docherty, A.C. Aiken, J.A. Huffman, I.M. Ulbrich, P.F. DeCarlo, D. Sueper, D.R. Worsnop, D.C. Snyder, R.E. Peltier, R.J. Weber, B.D. Grover, D.J. Eatough, B.J. Williams, A.H. Goldstein, P.J. Ziemann, and J.L. Jimenez. The 2005 Study of Organic Aerosols at Riverside (SOAR-1): Overview, Instrumental Intercomparisons, and Fine Particle Composition. *Atmospheric Chemistry and Physics*, 11, 12387-12420, doi:10.5194/acp-11-12387-2011, 2011.**
- D.V. Spracklen, J.L. Jimenez, K.S. Carslaw, D.R. Worsnop, M.J. Evans, G.W. Mann, Q. Zhang, M.R. Canagaratna, J. Allan, H. Coe, G. McFiggans, A. Rap and P. Forster. Aerosol mass spectrometer constraint on the global secondary organic aerosol budget. *Atmospheric Chemistry and Physics*, 11, 12109-12136, doi:10.5194/acp-11-12109-2011, 2011.
- Hodzic, C. Wiedinmyer, D. Salcedo, and J.L. Jimenez. Impact of Trash Burning on Air Quality in Mexico City. *Environmental Science and Technology*, 46, 4950-4957, doi:10.1021/es203954r, 2012.
- J.E. Thompson, P.L. Hayes, J.L. Jimenez, K. Adachi, X. Zhang, J. Liu, R.J. Weber, and P.R. Buseck. Aerosol Optical Properties at Pasadena, CA During CalNex 2010. *Atmospheric Environment*, 55, 190-200, doi:10.1016/j.atmosenv.2012.03.011, 2012.
- L.K. Sahu, Y. Kondo, N. Moteki, N. Takegawa, Y. Zhao, M.J. Cubison , J.L. Jimenez, S. Vay, G.S. Diskin, A. Wisthaler , T. Mikoviny, and L.G. Huey. Emission characteristics of black carbon in anthropogenic and biomass burning plumes over California during ARCTAS-CARB 2008. *Journal of Geophysical Research - Atmospheres*, 117, D16302, doi:10.1029/2011JD017401, 2012.
- R.H.H. Janssen, J. Vila-Guerau de Arellano, L.N. Ganzeveld, P. Kabat, J.L. Jimenez, D.K. Farmer, and C.C. van Heerwaarden. Combined effects of surface conditions, boundary layer dynamics and chemistry on diurnal SOA evolution. *Atmospheric Chemistry and Physics*, 12, 6827-6843, doi:10.5194/acp-12-6827-2012, 2012.

- D. Salcedo, A. Laskin, V. Shutthanandan, X. Querol, and J. L. Jimenez. Feasibility of trace element determination in particulate matter using online High Resolution Aerosol Mass Spectrometry. *Aerosol Science and Technology* 46:1187–1200, doi:10.1080/02786826.2012.701354, 2012.
- R. Zalakeviciute, M.L. Alexander, E. Allwine, J.L. Jimenez, B.T. Jobson, L.T. Molina, E. Nemitz, S.N. Pressley, T. VanReken, I.M. Ulbrich, E. Velasco and B.K. Lamb. Chemically-Resolved Aerosol Eddy Covariance Flux Measurements in Urban Mexico City during MILAGRO 2006. *Atmospheric Chemistry and Physics*, 12, 7809-7823, doi:10.5194/acp-12-7809-2012, 2012.
- X. Zhang, J. Liu, E.T. Parker, P.L. Hayes, J.L. Jimenez, J.A. de Gouw, J.H. Flynn, N. Grossberg, B.L. Lefer, R.J. Weber. On the Gas-Particle Partitioning of Soluble Organic Aerosol in Two Urban Atmospheres with Contrasting Emissions: Part 1. Bulk Water-Soluble Organic Carbon. *Journal of Geophysical Research - Atmospheres*, 117, D00V16, doi:10.1029/2012JD017908, 2012.
- H. Zhang, D.R. Worton, M. Lewandowski, J. Ortega, C.L. Rubitschun, J.H. Park, K. Kristensen, P. Campuzano-Jost, D.A. Day, J.L. Jimenez, M. Jaoui, J.H. Offenberg, T.E. Kleindienst, J. Gilman, W.C. Kuster, J. de Gouw, C.H. Park, G.W. Schade, A.A. Frossard, L. Russell, L. Kaser, W. Jud, A. Hansel, L. Cappellin, T. Karl, M. Glasius, A. Guenther, A.H. Goldstein, J.H. Seinfeld, A. Gold, R.M. Kamens, and J.D. Surratt. Organosulfates as Tracers for Secondary Organic Aerosol (SOA) Formation from 2-Methyl-3-Buten-2-ol (MBO) in the *Atmosphere. Environmental Science & Technology*, 46, 9437-9446, doi:10.1021/es301648z, 2012
- J. Liu, X. Zhang, E.T. Parker, P.R. Veres, J.M. Roberts, J. de Gouw, P.L. Hayes, J.L. Jimenez, J. Murphy, R. Ellis, L.G. Huey, R.J. Weber. On the Gas-Particle Partitioning of Soluble Organic Aerosol in Two Urban Atmospheres with Contrasting Emissions: Part 2. Gas and Particle Phase Formic Acid. *Journal of Geophysical Research - Atmospheres*, 117, D00V21, doi:10.1029/2012JD017912, 2012.
- B.L. van Drooge, M. Crusack, C. Reche, C. Mohr, A. Alastuey, X. Querol, A. Prevot, D.A. Day, J.L. Jimenez, and J.O. Grimalt. Molecular marker characterization of the organic composition of submicron aerosols from Mediterranean urban and rural environments under contrasting meteorological conditions. *Atmospheric Environment*, 61, 482-489, doi: 10.1016/j.atmosenv.2012.07.039, 2012.
- M.D. Jolleys, H. Coe, G. McFiggans, G. Capes, J.D. Allan, J. Crosier, P.I. Williams, G. Allen, K.N. Bower, J.L. Jimenez, L.M. Russell, M. Grutter, D. Baumgardner. Characterizing the Aging of Biomass Burning Organic Aerosol Using Mixing Ratios - a Meta-analysis of Four Regions. *Environmental Science & Technology*, 46, 13093–13102, DOI: 10.1021/es302386v, 2012.
- K.S. Docherty, M. Jaoui, E. Corse, J.L. Jimenez, J.H. Offenberg, M. Lewandowski, T.E. Kleindienst. Collection Efficiency of the Aerosol Mass Spectrometer for Chamber-Generated Secondary Organic Aerosols. *Aerosol Science and Technology*, 47, 294-309, DOI:10.1080/02786826.2012.752572, 2013.
- J. Ensberg, J. Craven, A. Metcalf, W. Angevine, R. Bahreini, J. Brioude, C. Cai, J. de Gouw, R. Ellis, J.H. Flynn, C. Haman, P. Hayes, J.L. Jimenez, B.L. Lefer, A. Middlebrook, J.

Murphy, J. Neuman, J. Nowak, J. Roberts, J. Stutz, P. Veres, J. Walker. Inorganic and black carbon aerosols in the Los Angeles Basin during CalNex. *Journal of Geophysical Research-Atmospheres*, 118, 1777-1803, doi:10.1029/2012JD018136, 2013.

- **P.L. Hayes, A.M. Ortega, M.J. Cubison, W.W. Hu, D.W. Toohey, J.H. Flynn, B.L. Lefer, N. Grossberg, S. Alvarez, B. Rappenglück, J.W. Taylor, J.D. Allan, J.S. Holloway, J.B. Gilman, W.C. Kuster, J.A. de Gouw, P. Massoli, X. Zhang, J. Liu, R.J. Weber, A.L. Corrigan, L.M. Russell, Y. Zhao, S.S. Cliff, G. Isaacman, D.R. Worton, N.M. Kreisberg, S.V. Hering, A.H. Goldstein, R. Thalman, E.M. Waxman, R. Volkamer, Y.H. Lin, J.D. Surratt, T.E. Kleindienst, J.H. Offenberg, K.D. Froyd, S. Dusanter, S. Griffith, P.S. Stevens, J. Brioude, W.M. Angevine, and J. L. Jimenez. Aerosol Composition and Sources in Los Angeles During the 2010 CalNex Campaign. *Journal of Geophysical Research-Atmospheres*, 118, 9233–9257, doi:10.1002/jgrd.50530, 2013.**
- F. Mei, P.L. Hayes, A. Ortega, J.W. Taylor, J.D. Allan, J. Gilman, W. Kuster, J. de Gouw, J.L. Jimenez, and J. Wang. Droplet activation properties of organic aerosols observed at an urban site during CalNex-LA. *Journal of Geophysical Research-Atmospheres*, 118, 2903–2917, doi:10.1002/jgrd.50285, 2013.
- T.B. Ryerson, A.E. Andrews, W.M. Angevine, T.S. Bates, C.A. Brock, B. Cairns, R.C. Cohen, O.R. Cooper, J.A. de Gouw, F.C. Fehsenfeld, R.A. Ferrare, M.L. Fischer, R.C. Flagan, A.H. Goldstein, J.W. Hair, R.M. Hardesty, C.A. Hostetler, J.L. Jimenez, A.O. Langford, E. McCauley, S.A. McKeen, L.T. Molina, A. Nenes, S.J. Oltmans, D.D. Parrish, J.R. Pederson, R.B. Pierce, K. Prather, P.K. Quinn, J.H. Seinfeld, C.J. Senff, A. Sorooshian, J. Stutz, J.D. Surratt, M. Trainer, R. Volkamer, E.J. Williams, and S.C. Wofsy. The 2010 California Research at the Nexus of Air Quality and Climate Change (CalNex) field study. *Journal of Geophysical Research-Atmospheres*, 118, 5830–5866, doi:10.1002/jgrd.50331, 2013.
- **D.K. Farmer, Q. Chen, J.R. Kimmel, K.S. Docherty, E. Nemitz, P.A. Artaxo, C.D. Cappa, S.T. Martin, and J.L. Jimenez. Chemically-resolved particle fluxes over tropical and temperate forests. *Aerosol Science and Technology*, 47, 818-830, DOI:10.1080/02786826.2013.791022, 2013.**
- R.H.H. Janssen, J. Vila-Guerau de Arellano, J.L. Jimenez, L. N. Ganzeveld, N.H. Robinson, J.D. Allan, H. Coe, and T.A.M. Pugh. Influence of meteorological forcings and isoprene chemistry on the organic aerosol budget in a tropical forest. *Journal of Geophysical Research-Atmospheres*, 118, 9351–9366, doi:10.1002/jgrd.50672, 2013.
- J.A. Huffman, C. Pöhlker, A.J. Prenni, P.J. DeMott, R.H. Mason, N.H. Robinson, J. Fröhlich-Nowoisky, Y. Tobo, V.R. Després, E. Garcia, D.J. Gochis, E. Harris, I. Müller-Germann, C. Ruzene, B. Schmer, B. Sinha, D.A. Day, M.O. Andreae, J.L. Jimenez, M. Galagher, S.M. Kreidenweis, A.K. Bertram, and U. Pöschl. High concentrations of biological aerosol particles and ice nuclei during and after rain. *Atmospheric Chemistry and Physics*, 13, 6151-6164, doi:10.5194/acp-13-6151-2013, 2013.
- **A.M. Ortega, D.A. Day, M.J. Cubison, W.H. Brune, D. Bon, J. de Gouw, and J.L. Jimenez. Secondary organic aerosol formation and primary organic aerosol oxidation**

from biomass-burning smoke in a flow reactor during FLAME-3. *Atmospheric Chemistry and Physics*, 13, 11551-11571, doi:10.5194/acp-13-11551-2013, 2013.

- W. Hu, M. Hu, B. Yuan, J.L. Jimenez, Q. Tang, J. Peng, W. Hu, M. Shao, M. Wang, L. Zeng, Y. Wu, Z. Gong, X. Huang, and L. He. Insights on organic aerosol aging and the influence of coal combustion at a regional receptor site of Central Eastern China. *Atmospheric Chemistry and Physics*, 13, 10095-10112, doi:10.5194/acp-13-10095-2013, 2013.
- L.H. Mielke, J. Stutz, C. Tsai, S.C. Hurlock, J.M. Roberts, P.R. Veres, K.D. Froyd, P.L. Hayes, M.J. Cubison, J.L. Jimenez, R.A.Washenfelder, C.J. Young, J.B. Gilman, J. de Gouw, J.H. Flynn, N. Grossberg, B.L. Lefer, J. Liu, R.J. Weber, and H.D. Osthoff. Nocturnal NOx reservoir species during Calnex-LA 2010. *Journal of Geophysical Research-Atmospheres*, 118, 10638–10652, doi:10.1002/jgrd.50783, 2013.
- R.E. O'Brien, T.B. Nguyen, A. Laskin, J. Laskin, P.L. Hayes, S. Liu, J.L. Jimenez, L.M. Russell, S.A. Nizkorodov, A.H. Goldstein. Probing Molecular Associations of Field-Collected and Laboratory-Generated SOA with Nano-DESI High-Resolution Mass Spectrometry. *Journal of Geophysical Research-Atmospheres*, 118, 1042–1051, doi:10.1002/jgrd.50119, 2013.
- W. Xiong, D.D. Hickstein, K.J. Schnitzenbaumer, J.L. Ellis, B.B. Palm, K.E. Keister, L. Miaja-Avila, G. Dukovic, J.L. Jimenez, M.M. Murnane, H.C. Kapteyn. Photoelectron spectroscopy of CdSe nanocrystals in the gas phase: a direct measure of the evanescent electron wavefunction of quantum dots. *Nano Letters*, 13, 2924–2930, doi:10.1021/nl401309z, 2013.
- A.W.H. Chan, G. Isaacman, K.R. Wilson, D.R. Worton, C.R. Ruehl, T. Nah, D.R. Gentner, T.R. Dallmann, T.W. Kirchstetter, R.A. Harley, J.B. Gilman, W.C. Kuster, J.A. de Gouw, J.H. Offenberg, T.E. Kleindienst, Y.H. Lin, C.L. Rubitschun, J.D. Surratt, P.L. Hayes, J.L. Jimenez, and A.H. Goldstein. Detailed Chemical Characterization of Unresolved Complex Mixtures in Atmospheric Organics: Insights into Emission Sources, Atmospheric Processing and Secondary Organic Aerosol Formation. *Journal of Geophysical Research-Atmospheres*, 118, 6783–6796, doi:10.1002/jgrd.50533, 2013.
- A.A. May, E.J.T. Levin, C.J. Hennigan, I. Riipinen, T. Lee, J.L. Collett, J.L. Jimenez, S.M. Kreidenweis, A.L. Robinson. Gas-particle partitioning of primary organic aerosol emissions. 3. Biomass burning. *Journal of Geophysical Research-Atmospheres*, 118, 11327–11338, doi:10.1002/jgrd.50828, 2013.
- J.S. Craven, A.R. Metcalf, R. Bahreini, A. Middlebrook, P.L. Hayes, H.T. Duong, A. Sorooshian, J.L. Jimenez, R.C. Flagan, and J.H. Seinfeld. Los Angeles Basin Airborne Organic Aerosol Characterization during CalNex. *Journal of Geophysical Research-Atmospheres*, 118, 11453–11467, doi:10.1002/jgrd.50853, 2013.
- **R. Li, B.B. Palm, A. Borbon, M. Graus, C. Warneke, A.M. Ortega, D.A. Day, W.H. Brune, J.L. Jimenez, and J.A. de Gouw. Laboratory studies on secondary organic aerosol formation from crude oil vapors. *Environmental Science & Technology*, 47, 12566–12574, doi:10.1021/es402265y, 2013.**
- H. Zhang, Z. Zhang, T. Cui, Y.H. Lin, N.A. Bhathela, J. Ortega, L. Cappellin, D.R. Worton, A.H. Goldstein, A. Guenther, J.L. Jimenez, A. Gold, and J.D. Surratt. Secondary Organic

Aerosol Formation from 2-Methyl-3-Buten-2-ol (MBO) Photooxidation: Evidence for Acid-Catalyzed Reactive Uptake of Epoxides. *Environmental Science & Technology Letters*, 1, 242–247, doi:10.1021/ez500055f, 2014.

- R. Holzinger, A.H. Goldstein, P.L. Hayes, J.L. Jimenez, and J. Timkovsky Chemical evolution of organic aerosol in Los Angeles during the CalNex 2010 study. Atmospheric Chemistry and Physics, 13, 10125-10141, doi:10.5194/acp-13-10125-2013, 2013.
- S. Carbone, M. Aurela, K. Saarnio, S. Saarikoski, A. Frey, D. Sueper, I.M. Ulbrich, J.L. Jimenez, M. Kulmala, D.R. Worsnop, and R. Hillamo. Wintertime aerosol chemistry in sub-Arctic urban air. *Aerosol Science and Technology*, 48, 313-323, DOI:10.1080/02786826.2013.875115, 2014.
- B.J. Williams, J.T. Jayne, A.T. Lambe, T. Hohaus, J.R. Kimmel, D. Sueper, W. Brooks, L.R. Williams, A.M. Trimborn, P.L. Hayes, J.L. Jimenez, N.M. Kreisberg, S.V. Hering, D.R. Worton, A.H. Goldstein, D.R. Worsnop. The First Combined Thermal Desorption Aerosol Gas Chromatograph - Aerosol Mass Spectrometer (TAG-AMS). *Aerosol Science and Technology*, 48, 358-370, doi:10.1080/02786826.2013.875114, 2014.
- S. Philip, R.V. Martin, J.R. Pierce, J.L. Jimenez, Q. Zhang, M.R. Canagaratna, D.V. Spracklen, C.R. Nowlan, L.N. Lamsal, M.J. Cooper, and N. A. Krotkov. Spatially and seasonally resolved estimate of the ratio of organic matter to organic carbon. *Atmospheric Environment*, 87, 34-40, doi:10.1016/j.atmosenv.2013.11.065, 2014.
- **R.L.N. Yatavelli, H. Stark, S.L. Thompson, J.R. Kimmel, M.J. Cubison, D.A. Day, P. Campuzano-Jost, B.B. Palm, A. Hodzic, J.A. Thornton, J.T. Jayne, D.R. Worsnop, and J.L. Jimenez. Semi-Continuous Measurements of Gas-Particle Partitioning of Organic Acids in a Ponderosa Pine Forest Using a MOVI-HRToF-CIMS. *Atmospheric Chemistry and Physics*, 14, 1527-1546, doi:10.5194/acp-14-1527-2014, 2014.**
- J.J. Ensberg, P.L. Hayes, J.L. Jimenez, J.B. Gilman, W.C. Kuster, J.A. de Gouw, J.S. Holloway, T.D. Gordon, S. Jathar, A.L. Robinson, and J.H. Seinfeld. Emission Factor Ratios, SOA Mass Yields, and the Impact of Vehicular Emissions on SOA Formation. *Atmospheric Chemistry and Physics*, 14, 2383-2397, doi:10.5194/acp-14-2383-2014, 2014.
- D.D. Hickstein, F. Dollar, J.L. Ellis, K.J. Schnitzenbaumer, K.E. Keister, G.M. Petrov, C. Ding, B.B. Palm, J.A. Gaffney, M.E. Foord, S.B. Libby, G. Dukovic, J.L. Jimenez, H.C. Kapteyn, M.M. Murnane, and W. Xiong. Mapping nanoscale absorption of femtosecond laser pulses using plasma explosion imaging. *ACS Nano*, 8, 8810–8818, doi:10.1021/nn503199v, 2014.
- M. Pandolfi, X. Querol, A. Alastuey, J.L. Jimenez, O. Jorba, D. Day, A. Ortega, M.J. Cubison, A. Comerón, M. Sicard, C. Mohr, A.S.H. Prévôt, M.C. Minguillón, J. Pey, J.M. Baldasano, J.F. Burkhart, R. Seco, J. Peñuelas, B.L. van Drooge , B. Artiñano, C. Di Marco, E. Nemitz, S. Schallhart, A. Metzger, A. Hansel, J. Llorente, S. Ng, J. Jayne, S. Szidat. Effects of Sources and Meteorology on Particulate Matter in the Western Mediterranean Basin: An overview of the DAURE campaign. *Journal of Geophysical Research-Atmospheres*, 119, 4978–5010, doi:10.1002/2013JD021079, 2014.
- M. Crippa, F. Canonaco, V.A. Lanz, M. Äijälä, J.D. Allan, S. Carbone, G. Capes, M. Dall'Osto, D.A. Day, P.F. DeCarlo, M. Ehn, A. Eriksson, E. Freney, L. Hildebrandt Ruiz, R. Hillamo, J.L. Jimenez, H. Junninen, A. Kiendler-Scharr, A.-M. Kortelainen, M. Kulmala, A.

Laaksonen, A.A. Mensah, C. Mohr, E. Nemitz, C. O'Dowd, J. Ovadnevaite, S.N. Pandis, T. Petäjä, L. Poulain, S. Saarikoski, K. Sellegri, E. Swietlicki, P. Tiitta, D.R. Worsnop, U. Baltensperger, and A.S.H. Prévôt. Organic aerosol components derived from 25 AMS data sets across Europe using a consistent ME-2 based source apportionment approach. *Atmospheric Chemistry and Physics*, 14, 6159-6176, doi:10.5194/acp-14-6159-2014, 2014.

- J. Ortega, A. Turnipseed, A.B. Guenther, T.G. Karl, D.A. Day, D. Gochis, J.A. Huffman, A.J. Prenni, E.J.T. Levin, S.M. Kreidenweis, P.J. DeMott, Y. Tobo, E.G. Patton, A. Hodzic, Y. Cui, P.C. Harley, R.S. Hornbrook, E.C. Apel, R.K. Monson, A.S.D. Eller, J.P. Greenberg, M.C. Barth, P. Campuzano-Jost, B.B. Palm, J.L. Jimenez, A.C. Aiken, M.K. Dubey, C. Geron, J. Offenberg, M.G. Ryan, P.J. Fornwalt, S.C. Pryor, F.N. Keutsch, J.P. DiGangi, A.W.H. Chan, A.H. Goldstein, G.M. Wolfe, S. Kim, L. Kaser, R. Schnitzhofer, A. Hansel, C.A. Cantrell, R.L. Mauldin, J.N. Smith. Overview of the Manitou Experimental Forest Observatory: Site description and selected science results from 2008-2013. *Atmospheric Chemistry and Physics*, 14, 6345-6367, doi:10.5194/acp-14-6345-2014, 2014.
- P. Zotter, I. El-Haddad, Y. Zhang, P.L. Hayes, X. Zhang, Y.H. Lin, L. Wacker, J. Schnelle-Kreis, G. Abbaszade, R. Zimmermann, J.D. Surratt, R. Weber, J.L. Jimenez, S. Szidat, U. Baltensperger, A.S.H. Prévôt. Diurnal cycle of fossil and non-fossil carbon using radiocarbon analyses during CalNex. *Journal of Geophysical Research-Atmospheres*, 119, 6818–6835, doi:10.1002/2013JD021114, 2014
- S. Saarikoski, P. Keronen, S. Carbone, C. Sioutas, M.J. Cubison, D.R. Worsnop, J.L. Jimenez, and R. Hillamo. Evaluation of the performance of a particle concentrator for on-line instrumentation. *Atmospheric Measurement Techniques*, 7, 2121-2135, doi:10.5194/amt-7-2121-2014, 2014.
- L.E. Hatch, K.A. Pratt, J.A. Huffman, J.L. Jimenez, and K.A. Prather. Impacts of aerosol aging on laser desorption/ionization in single-particle mass spectrometers. *Aerosol Science and Technology*, 48, 1050-1058, doi:10.1080/02786826.2014.955907, 2014.
- J.D. Fast, J. Allan, R. Bahreini, J. Craven, L. Emmons, R. Ferrare, P. L. Hayes, A. Hodzic, J. Holloway, C. Hostetler, J.L. Jimenez, H. Jonsson, S. Liu, Y. Liu, A. Metcalf, A. Middlebrook, J. Nowak, M. Pekour, A. Perring, L. Russell, A. Sedlacek, J. Seinfeld, A. Setyan, J. Shilling, M. Shrivastava, S. Springston, C. Song, R. Subramanian, J.W. Taylor, V. Vinoj, Q. Yang, R.A. Zaveri, and Q. Zhang. Modeling Regional Aerosol Variability over California and Its Sensitivity to Emissions and Long-Range Transport during the 2010 CalNex and CARES Campaigns. *Atmospheric Chemistry and Physics*, 14, 10013-10060, doi:10.5194/acp-14-10013-2014, 2014.
- K. Tsigaridis, N. Daskalakis, M. Kanakidou, P.J. Adams, P. Artaxo, R. Bahadur, Y. Balkanski, S.E. Bauer, N. Bellouin, A. Benedetti, T. Bergman, T.K. Berntsen, J.P. Beukes, H. Bian, K.S. Carslaw, M. Chin, G. Curci, T. Diehl, R. C. Easter, S.J. Ghan, S.L. Gong, A. Hodzic, C.R. Hoyle, T. Iversen, S. Jathar, J.L. Jimenez, J.W. Kaiser, A. Kirkevåg, D. Koch, H. Kokkola, Y.H. Lee, G. Lin, X. Liu, G. Luo, X. Ma, G.W. Mann, N. Mihalopoulos, J.-J. Morcrette, J.-F. Müller, G. Myhre, S. Myriokefalitakis, S. Ng, D. O'Donnell, J.E. Penner, L. Pozzoli, K.J. Pringle, L.M. Russell, M. Schulz, J. Sciare, Ø. Seland, D.T. Shindell, S. Sillman, R.B. Skeie, D. Spracklen, T. Stavrakou, S.D. Steenrod, T. Takemura, P. Tiitta, S. Tilmes, H. Tost, T. van Noije, P.G. van Zyl, K. von Salzen, F. Yu, Z. Wang, Z. Wang, R.A.

Zaveri, H. Zhang, K. Zhang, Q. Zhang, X. Zhang. The AeroCom evaluation and intercomparison of organic aerosol in global models. *Atmospheric Chemistry and Physics*, 14, 10845-10895, doi:10.5194/acp-14-10845-2014, 2014.

- C. Knote, A. Hodzic, J.L. Jimenez, R.M. Volkamer, J.J. Orlando, S. Baidar, J. Brioude, J. Fast, D.R. Gentner, A. Goldstein, P.L. Hayes, W.B. Knighton, H. Oetjen, A. Setyan, H. Stark, R. Thalman, G. Tyndall, R. Washenfelder, E. Waxman, and Q. Zhang. Simulation of semi-explicit mechanisms of SOA formation from glyoxal in aerosol in a 3D model. *Atmospheric Chemistry and Physics*, 14, 6213-6239, doi:10.5194/acp-14-6213-2014, 2014.
- **R. Li, W.H. Brune, B.B. Palm, A.M. Ortega, J. Hlywiak, W. Hu, Z. Peng, D.A. Day, C. Knote, J. de Gouw, and J. L. Jimenez. Modeling the radical chemistry in an Oxidation Flow Reactor: radical formation and recycling, sensitivities, and OH exposure estimation equation. *Journal of Physical Chemistry A*, 119, 4418–4432, doi:10.1021/jp509534k, 2015.**
- **P.L. Hayes, A.G. Carlton, K.R. Baker, R. Ahmadov, R.A. Washenfelder, S. Alvarez, B. Rappenglück, J.B. Gilman, W.C. Kuster, J.A. de Gouw, P. Zotter, A.S.H. Prévôt, S. Szidat, T.E. Kleindienst, J.H. Offenberg, and J.L. Jimenez. Modeling the formation and aging of secondary organic aerosols in Los Angeles during CalNex 2010. *Atmospheric Chemistry and Physics*, 15, 5773-5801, doi:10.5194/acp-15-5773-2015, 2015**

Papers Under Review:

A.M. Ortega, P.L. Hayes, Z. Peng, B.B. Palm, W. Hu, D.A. Day, R. Li, M.J. Cubison, W.H. Brune, M. Graus, C. Warneke, J.B. Gilman, W.C. Kuster, J. de Gouw, and J.L. Jimenez. Real-time Measurements of Secondary Organic Aerosol Formation and Aging from Ambient Air in an Oxidation Flow Reactor in the Los Angeles Area. *Atmospheric Chemistry and Physics Discussions*, 15, 21907-21958, doi:10.5194/acpd-15-21907-2015, 2015.